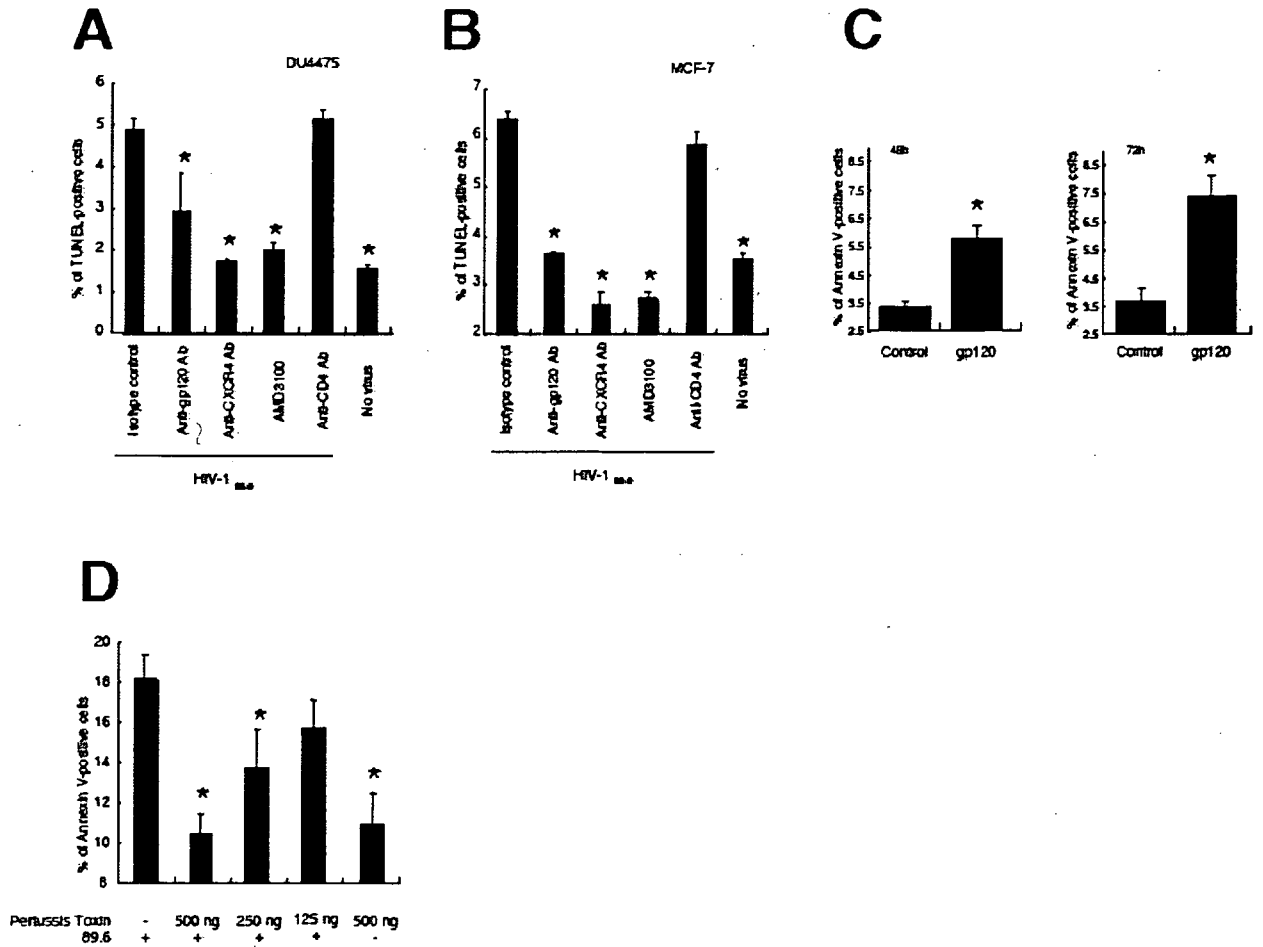

Fig. (4). HIV-1 induces breast cancer cell apoptosis through Env-CXCR4 interaction. DU4475 (**A**) and MCF-7 (**B**) cells were preincubated with 20 μl of the anti-CD4 antibody (Leu-3a), 5 μg of the anti-CXCR4 antibody (12G5), or 2 μM CXCR4 antagonist (AMD3100) and then inoculated with HIV-$1_{89.6}$ (100 ng of the HIV-1 p24 antigen). To prevent gp120-CXCR4 interaction, the virus that was preincubated with 5 μg of the cross-reactive anti-gp120 antibody was also used. After a 36h incubation, the cells were subjected to TUNEL assay to determine the percentage of apoptotic cells (*$p<0.01$ compared with the isotype control group (Dunnett's test following ANOVA)). (**C**) Apoptosis of MCF-7 cells after 48h or 72h of coculture with HEK293 cells transfected with vector-derived mRNA (control) or mRNA encoding HIV-$1_{89.6}$ gp120. MCF-7 cells were subjected to Annexin-V staining assay (*$P<0.01$ *vs* control, unpaired t test). (**D**) To investigate whether intracellular signaling is involved in HIV-1-associated breast cancer cell apoptosis, MCF-7 cells were preincubated with increasing concentrations of pertussis toxin, and inoculated with HIV-$1_{89.6}$. After a 36h incubation, the cells were subjected to Annexin-V staining assay (*$p<0.01$ compared with the control group without pertussis toxin (Dunnett's test following ANOVA)).

mediated apoptosis requires $G_{i\alpha}$ protein signaling in breast cancer cells (Fig. **4D**).

Conformational Heterogeneity of CXCR4 on Cell Surface

To characterize CXCR4 on breast cancer and T cells, three conformation-specific anti-CXCR4 mAbs (12G5, 44717.111, and IA2-F9; [31, 35]) were used for flow cytometric analysis (Fig. **5**). 12G5 recognizes a determinant in the first and second extracelullar loops of CXCR4, and 44717.111 recognizes a determinant in the second extracelullar loop (ECL-2) of CXCR4. Furthermore, IA2-F9 was previously generated in our laboratory by the immunization with a synthetic cyclic peptide that mimics the conformational specific domain of CXCR4 (UPA: Asn_{176} to Ile_{185}). In breast cancer cells (DU4475 and MCF-7) and T cell (Molt4#8), an anti-CXCR4 *N*-terminal rabbit polyclonal antibody (Fig. **1A**) and IA2F9 (Fig. **5A,B**) show almost equal reactivity. On the other hand, 12G5 and 44717.111 show high reactivity against CXCR4 on Molt4#8 cells but not on cells of breast cancer cell lines (Fig. **5A**). Furthermore, other breast cancer cell lines (MDA-MB-231 and MDA-MB-453) were also analyzed for CXCR4 expression by flow cytometric analysis. As expected, 12G5 and 44717.111 hardly react with CXCR4 on cells of both cell lines (Fig. **5B**). Taken together, these results suggest that both epitopes of 12G5 and 44717.111 are masked in breast cancer cells and that conformational differences in the microenvironment around ECL-2 plays an important role in the induction of HIV-1 gp120/CXCR4-mediated breast cancer apoptosis without CD4-induced conformational changes of gp120.

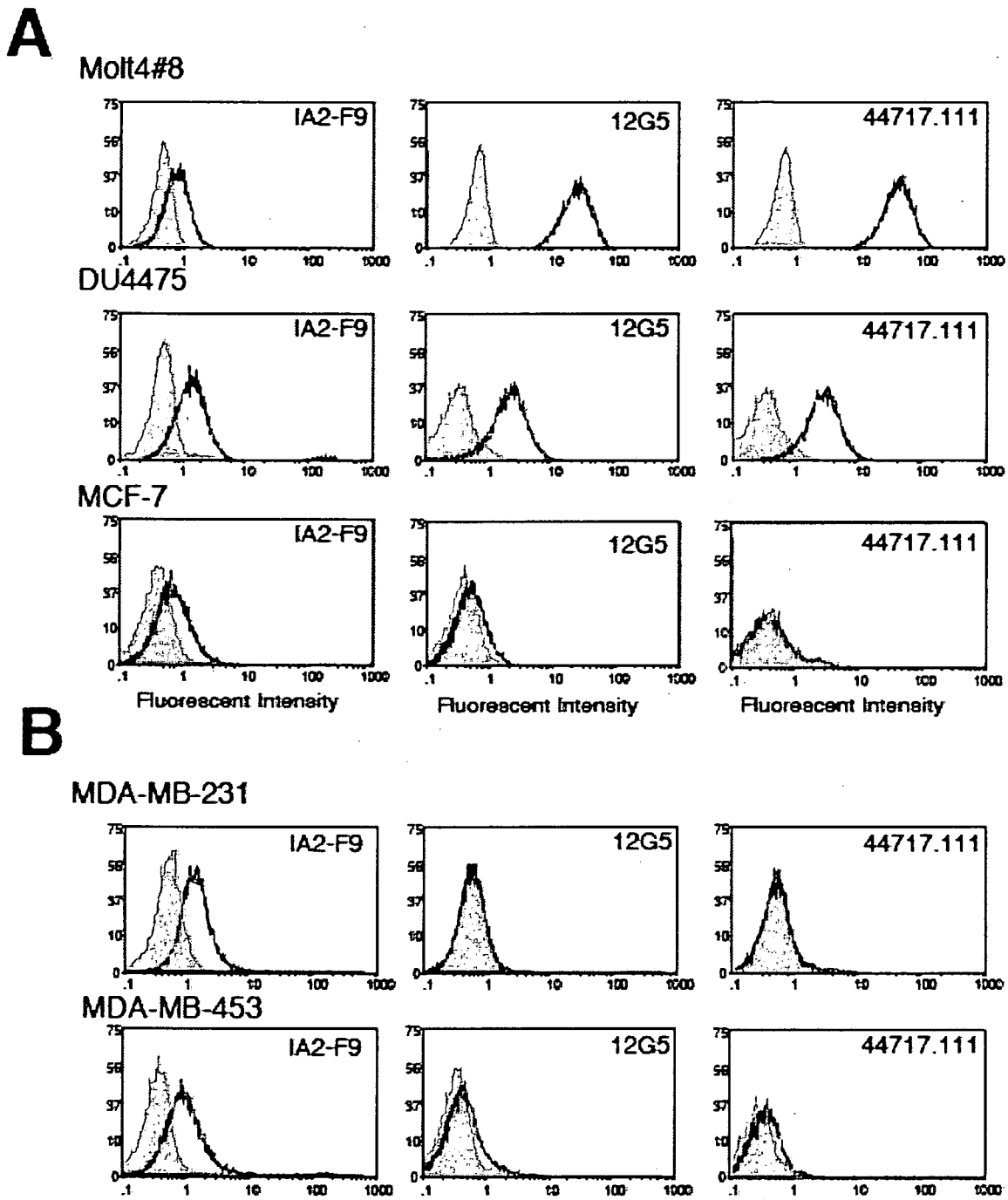

Fig. (5). Binding profile of conformation-specific anti-CXCR4 antibodies to T cell line and breast cancer cell lines. Human T-cell line (A, Molt4#8) and breast cancer cell lines (A, DU4475 and MCF-7; B, MDA-MB-231 and MDA-MB-453) were incubated with 10 μg/ml conformation-specific anti-CXCR4 antibodies (12G5, 44717.111, and IA2F9; red line), or isotype control (blue line). Subsequently, cells were incubated with suitable FITC-labeled secondary antibodies, and subjected to flow cytometry.

HIV-Induced Apoptosis of Breast Cancer Cells *Via* CXCR4 is Mediated by gp120 But Does Not Require CD4-Induced Conformational Change of gp120

Because DU4475 and MCF-7 cells do not express CD4 (Fig. **1B**), we hypothesized that mutant gp120 (E370R) with a low CD4 binding ability [36] can specifically induce the apoptosis of breast cancer cells. To test this hypothesis, gp120 (E370R)-expressing HEK293 cells were cocultured with MCF-7 or CEM cells. As expected, gp120 (E370R) can specifically induced the apoptosis of breast cancer cells (Fig. **6**). This result indicates that the HIV-induced apoptosis of breast cancer cells *via* CXCR4 does not require a CD4-induced conformational change of gp120.

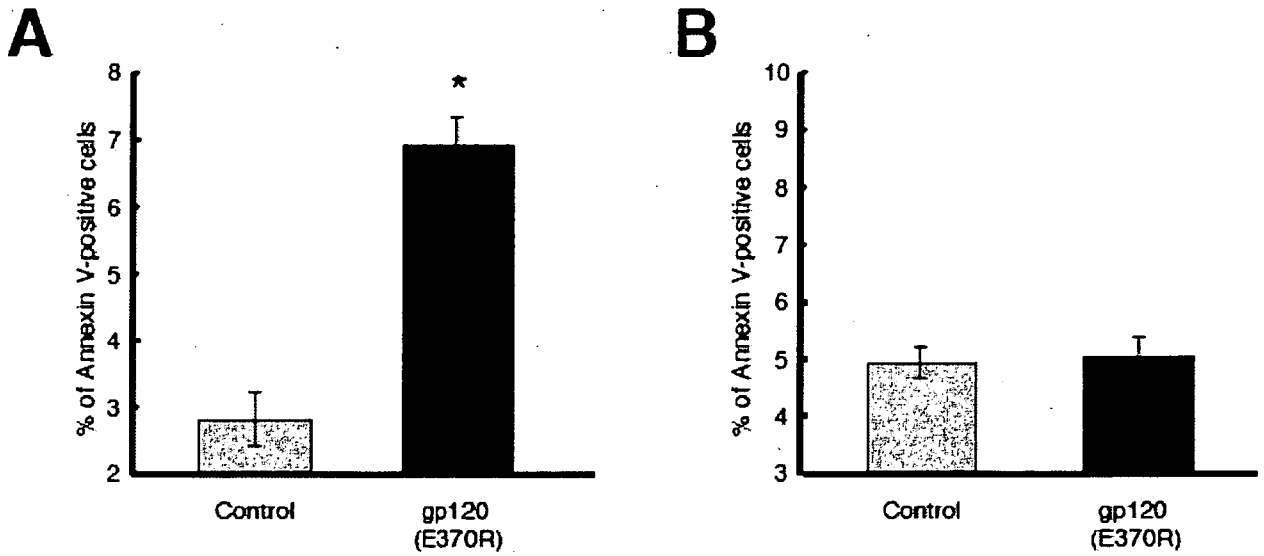

Fig. (6). CD4-induced conformational change in gp120 is not required to induce the apoptosis of breast cancer cells. Mutant gp120 (E370R, black) expressing and mock cells (gray) were seeded on polycarbonate Transwell filter inserts and cocultured with MCF-7 (**A**) or CEM (**B**) in the lower chamber. After 48h of coculture, MCF-7 cells or CEM cells were subjected to Annexin-V staining assay.

DISCUSSION

Because immunodeficiency fails to provide protection against viral infection or viral reactivation, the relative risks of HIV-1-associated cancers, particularly human-herpesvirus-8-associated Kaposi's sarocoma, and Epstein-Barr-virus-associated non-Hodgkin lymphoma, increase in HIV-1-infected patients [37-39]. On the other hand, the low incidence of breast cancer among HIV-1-infected patients has been reported by investigators from both African and Western countries [11, 41]. Several hypotheses explaining the low incidence of breast cancer among HIV-1-infected patients have been proposed (e.g., immunodeficiency, socioeconomic state, racial disparity, metabolic complications of antiretroviral therapy, and short life span of HIV-1-infected patients) [10-15]. On the basis of our data, we cannot exclude the possibility that HIV-1-induced breast cancer cell apoptosis is responsible for the reduced risk of breast cancer among HIV-1-infected patients, although further investigation is required.

In HIV-1-infected patients, soluble gp120 secreted by infected cells and gp120 expressed on virions or on the cell surface of infected cells can induce the apoptosis of uninfected T-cells [22]. The secreted and expressed gp120 can be considered as a ligand of CD4 and coreceptor molecules and may be involved in CD4- or CCR5-mediated Fas-dependent and CXCR4-mediated Fas-independent apoptosis [22]. As shown in Fig. 1, CXCR4 is expressed on human breast cancer cells; however, CD4 is hardly expressed. A recent study has shown that the degree of apoptosis of bystander T-cells induced by HIV-1 is associated with gp120-receptor affinity [25]. Therefore, we investigated whether HIV-1 can directly mediate the apoptosis of CD4-negative breast cancer cells. Our study showed that the induction of the apoptosis of breast cancer cells by HIV-1 is dependent on the viral strain. The laboratory-adapted and primary R5X4 and X4 viral isolates induced a high degree of apoptosis but not the R5 viral isolate.

We further demonstrated that the HIV-1-mediated apoptosis of breast cancer cells can be inhibited by using an anti-CXCR4 antibody and AMD3100. This indicates that CXCR4 is the major determinant of the HIV-1-induced apoptosis of breast cancer cells. Although Holm *et al.* proposed that the degree of apoptosis of bystander T-cells induced by HIV-1 is also associated with the coreceptor binding site exposure of gp120 induced by CD4 [25], breast cancer cell lines do not express CD4 molecules on the cell surface. However, as shown in Fig. **5**, the conformational differences in the microenvironment around ECL-2 of CXCR4 on breast cancer cells may contribute to the direct gp120-CXCR4 interaction without the coreceptor binding site exposure of gp120.

As a type of effective oncolytic virotherapy for breast cancer, HIV-1 may be used to destroy breast cancer cells without harming healthy cells. To test this possibility, we prepared aldrithiol-2 (AT-2)-inactivated HIV-1 that has functional envelope glycoproteins but is not infectious. Interestingly, Annexin-V staining assay indicated that the percentage of apoptotic breast cancer cells significantly increased following the inoculation of AT-2-inactivated HIV-$1_{89.6}$ (data not shown). However, it is difficult to use AT-2-inactivated HIV-1 for practical applications. Therefore, further structural optimization for mutant gp120 (E370R) that specifically induces the apoptosis of breast cancer cells may provide more efficient therapeutic information for developing a novel HIV-based breast cancer therapy.

At least 23 types of cancer cell express CXCR4 [41]. In addition, the relative risks of prostate, and bladder and breast cancer are significantly low in HIV-1-infected patients [36, 38]. Therefore, the low incidences of these cancers among HIV-1-infected patients may be involved in the emergence of R5X4 and X4 viruses *in vivo*. Further investigation of the effects of HIV-1 on these cancer cell types is necessary for elucidating the pathology of cancers and developing a novel HIV-based cancer therapy.

ACKNOWLEDGEMENTS

We thank the NIH AIDS Research and Reference Reagent Program for providing primary HIV-1 isolates (HIV-1_{MJ4}, HIV-$1_{92UG029}$, and HIV-$1_{98IN017}$), and AMD3100. We also thank the Cell Resource Center for Biomedical Research, Tohoku University for providing the breast cancer cell lines MCF-7, and SK-BR-3. This study was supported in part by a Grant-in-Aid for Scientific Research from the Ministry of Education, Culture, Sports, Science and Technology of Japan, and a Health Science Research Grant from the Ministry of Health, Labour, and Welfare of Japan.

REFERENCES

[1] Fauci AS. The human immunodeficiency virus: infectivity and mechanisms of pathogenesis. Science 1988; 239: 617-622.

[2] McCune JM. The dynamics of CD4+ T-cell depletion in HIV disease. Nature 2001; 410: 974-979.

[3] Rabkin CS. AIDS and cancer in the era of highly active antiretroviral therapy (HAART). Eur J Cancer 2001; 37: 1316-1319.

[4] Spano JP, Atlan D, Breau JI *et al.* AIDS and non-AIDS-related malignancies: a new vexing challenge in HIV-positive patients. Part I: Kaposi's sarcoma, non-Hodgkin's lymphoma, and Hodgkin's lymphoma. Eur J Intern Med 2002; 13: 170-179.

[5] Goedert JJ, Cote TR, Virgo P *et al.* Spectrum of AIDS-associated malignant disorders. Lancet 1998; 351: 1833-1839.

[6] Phelps RM, Smith DK, Heilig CM *et al.* Cancer incidence in women with or at risk for HIV. Int J Cancer 2001; 94: 753-757.

[7] Mbulaiteye SM, Biggar RJ, Goedert JJ *et al.* Immune deficiency and risk for malignancy among persons with AIDS. J Acquir Immune Defic Syndr 2003; 32: 527-533.

[8] Remick SC. Non-AIDS-defining cancers. Hematol Oncol Clin North Am 1996; 10: 1203-1213.

[9] Grulich AE, Li Y, McDonald A *et al.* Rates of non-AIDS-defining cancers in people with HIV infection before and after AIDS diagnosis. Aids 2002; 16: 1155-1161.

[10] Herida M, Mary-Krause M, Kaphan R *et al.* Incidence of non-AIDS-defining cancers before and during the highly active antiretroviral therapy era in a cohort of human immunodeficiency virus-infected patients. J Clin Oncol 2003; 21: 3447-3453.

[11] Amir H, Kaaya EE, Kwesigabo G *et al.* Breast cancer before and during the AIDS epidemic in women and men: a study of Tanzanian Cancer Registry Data 1968 to 1996. J Natl Med Assoc 2000; 92: 301-305.

[12] Pantanowitz L, Dezube BJ. Reasons for a deficit of breast cancer among HIV-infected patients. J Clin Oncol 2004; 22: 1347-1348.

[13] Dong KL, Bausserman LL, Flynn MM *et al.* Changes in body habitus and serum lipid abnormalities in HIV-positive women on highly active antiretroviral therapy (HAART). J Acquir Immune Defic Syndr 1999; 21: 107-113.

[14] Schreier LE, Berg GA, Basilio FM *et al.* Lipoprotein alterations, abdominal fat distribution and breast cancer. Biochem Mol Biol Int 1999; 47: 681-690.

[15] Krown SE. Breast cancer in the setting of HIV infection: cause for concern? Cancer Invest 2002; 20(4): 590-592.

[16] Moore JP, Trkola A, Dragic T. Co-receptors for HIV-1 entry. Curr Opin Immunol 1997; 9: 551-562.

[17] Feng Y, Broder CC, Kennedy PE *et al.* HIV-1 entry cofactor: functional cDNA cloning of a seven-transmembrane, G protein-coupled receptor. Science 1996; 272: 872-877.

[18] Connor RI, Sheridan KE, Ceradini D *et al.* Change in coreceptor use coreceptor use correlates with disease progression in HIV-1--infected individuals. J Exp Med 1997; 185: 621-628.

[19] Scarlatti G, Tresoldi E, Bjorndal A *et al. In vivo* evolution of HIV-1 co-receptor usage and sensitivity to chemokine-mediated suppression. Nat Med 1997; 3: 1259-1265.

[20] Weissman D, Rabin RL, Arthos J *et al.* Macrophage-tropic HIV and SIV envelope proteins induce a signal through the CCR5 chemokine receptor. Nature 1997; 389: 981-985.

[21] Algeciras-Schimnich A, Vlahakis SR, Villasis-Keever A *et al.* CCR5 mediates Fas- and caspase-8 dependent apoptosis of both uninfected and HIV infected primary human CD4 T cells. AIDS 2002; 16: 1467-1478.

[22] Ahr B, Robert-Hebmann V, Devaux C *et al.* Apoptosis of uninfected cells induced by HIV envelope glycoproteins. Retrovirology 2004; 1:12.

[23] Berndt C, Mopps B, Angermuller S *et al.* CXCR4 and CD4 mediate a rapid CD95-independent cell death in CD4(+) T cells. Proc Natl Acad Sci USA 1998; 95: 12556-12561.

[24] Kreisberg JF, Kwa D, Schramm B *et al.* Cytopathicity of human immunodeficiency virus type 1 primary isolates depends on coreceptor usage and not patient disease status. J Virol 2001; 75: 8842-8847.

[25] Holm GH, Zhang C, Gorry PR *et al.* Apoptosis of bystander T cells induced by human immunodeficiency virus type 1 with increased envelope/receptor affinity and coreceptor binding site exposure. J Virol 2004; 78: 4541-4551.

[26] Herbein G, Mahlknecht U, Batliwalla F *et al.* Apoptosis of CD8+ T cells is mediated by macrophages through interaction of HIV gp120 with chemokine receptor CXCR4. Nature 1998; 395: 189-194.

[27] Penn ML, Grivel JC, Schramm B *et al.* CXCR4 utilization is sufficient to trigger CD4+ T cell depletion in HIV-1-infected human lymphoid tissue. Proc Natl Acad Sci USA 1999; 96: 663-668.

[28] Jekle A, Schramm B, Jayakumar P *et al.* Coreceptor phenotype of natural human immunodeficiency virus with nef deleted evolves *in vivo*, leading to increased virulence. J Virol 2002; 76: 6966-6973.

[29] Muller A, Homey B, Soto H *et al.* Involvement of chemokine receptors in breast cancer metastasis. Nature 2001; 410: 50-56.

[30] Kato M, Kitayama J, Kazama S *et al.* Expression pattern of CXC chemokine receptor-4 is correlated with lymph node metastasis in human invasive ductal carcinoma. Breast Cancer Res 2003; 5: R144-150.

[31] Misumi S, Endo M, Mukai R *et al.* A novel cyclic peptide immunization strategy for preventing HIV-1/AIDS infection and progression. J Biol Chem 2003; 278: 32335-32343.

[32] Remick SC, Harper GR, Abdullah MA *et al.* Metastatic breast cancer in a young patient seropositive for human immunodeficiency virus. J Natl Cancer Inst 1991; 83: 447-448.

[33] Samuelsson A, Brostrom C, van Dijk N *et al.* Apoptosis of CD4+ and CD19+ cells during human immunodeficiency virus type 1 infection--correlation with clinical progression, viral load, and loss of humoral immunity. Virology 1997; 238: 180-188.

[34] Vlahakis SR, Villasis-Keever A, Gomez TS *et al.* Human immunodeficiency virus-induced apoptosis of human hepatocytes *via* CXCR4. J Infect Dis 2003; 188: 1455-1460.

[35] Baribaud F, Edwards TG, Sharron M *et al.* Antigenically distinct conformations of CXCR4. J Virol 2001; 75: 8957-8967.

[36] Olshevsky U, Helseth E, Furman C *et al.* Identification of individual human immunodeficiency virus type 1 gp120 amino acids important for CD4 receptor binding. J Virol 1990; 64: 5701-5707.

[37] Gallagher B, Wang Z, Schymura MJ *et al.* Cancer incidence in New York State acquired immunodeficiency syndrome patients. Am J Epidemiol 2001; 154: 544-556.

[38] Biggar RJ, Kirby KA, Atkinson J *et al.* Cancer risk in elderly persons with HIV/AIDS. J Acquir Immune Defic Syndr 2004; 36: 861-868.

[39] Frisch M, Biggar RJ, Engels EA *et al.* Association of cancer with AIDS-related immunosuppression in adults. JAMA 2001; 285: 1736-1745.

[40] Pantanowitz L, Dezube BJ. Breast cancer in women with HIV/AIDS. JAMA 2001; 285: 3090-3091.

[41] Balkwill F. The significance of cancer cell expression of the chemokine receptor CXCR4. Semin Cancer Biol 2004; 14: 171-179.

Received: July 5, 2007 **Revised: September 5, 2007** **Accepted: September 5, 2007**

ELSEVIER

INSTITUT PASTEUR

Microbes and Infection xx (2007) 1–8

www.elsevier.com/locate/micinf

Original article

HIV-1 production is specifically associated with human NMT1 long form in human NMT isozymes

Nobutoki Takamune, Kayoko Gota, Shogo Misumi, Kenzo Tanaka, Shigetaka Okinaka, Shozo Shoji*

Department of Pharmaceutical Biochemistry, Faculty of Medical and Pharmaceutical Sciences, Kumamoto University, 5-1 Oe-Honmachi, Kumamoto 862-0973, Japan

Received 29 August 2007; accepted 28 October 2007

Abstract

The *N*-myristoylation of the N-terminal of human immunodeficiency virus type-1 (HIV-1) $Pr55^{gag}$ by human *N*-myristoyltransferase (hNMT) is a prerequisite modification for HIV-1 production. hNMT consists of multiple isozymes encoded by *hNMT1* and *hNMT2*. The hNMT1 isozyme consists of long, medium, and short forms. Here, we investigated which isozyme is crucial for HIV-1 production. Human embryonic kidney (HEK) 293 cells transfected with infectious HIV-1 vectors were used as models of HIV-1-infected cells in this study. The significant reduction in HIV-1 production and the failure of the specific localization of $Pr55^{gag}$ in a detergent-resistant membrane fraction were dependent on the knockdown of the different forms of the hNMT1 isozyme but not of the hNMT2 isozyme. Additionally, the coexpression of an inactive mutant hNMT1 isozyme, namely the hNMT1 long form ($hNMT1_L$), but not that of other hNMT mutants resulted in a significant reduction in HIV-1 production. These results strongly suggest that HIV-1 production is specifically associated with hNMT1, particularly $hNMT1_L$, but not with hNMT2 *in vivo*, contributing to the understanding of a step in HIV-1 replication.

Keywords: *N*-Myristoyltransferase; Human immunodeficiency virus type-1

1. Introduction

N-Myristoyltransferase (NMT) (EC 2.3.1.9.7) mainly catalyzes the covalent attachment of myristate from myristoyl coenzyme A to the α-amino group of N-terminal Gly of nascent or proteolytic processed proteins [1–3]; this modification is called protein *N*-myristoylation [4]. *N*-Myristoylation is important as a main membrane-targeting signal of modified proteins [5]. The consensus sequence of peptide substrates for NMT is generally Gly-X-X-X-Ser/Thr, in which N-terminal Gly is absolutely required and Ser/Thr at position five is preferred [1,2].

N-Myristoylation is essential for modified proteins to function appropriately. Many viral proteins in addition to cellular proteins can be *N*-myristoylated [6]. *N*-Myristoylation occurs in products from the human immunodeficiency virus type-1 (HIV-1) genome: the N-terminal Gly of $Pr55^{gag}$ [7–9] and Nef [10]. $Pr55^{gag}$ is a structural protein of HIV-1 and *N*-myristoylation of $Pr55^{gag}$ is essential for the release of HIV-1 virions and HIV-1 infectivity [7–9,11,12]. The *N*-myristoyl group promotes the targeting of $Pr55^{gag}$ to the plasma membrane, particularly the detergent-resistant membrane (DRM), which is thought to be closely associated with $Pr55^{gag}$ assembly, followed by the budding of infectious viral particles [13–15].

Mammalian NMTs, particularly those in humans, mice, rats, and bovine, appear to be encoded by two genes: *NMT1* and *NMT2* [16–18]. Furthermore, human NMT1 (hNMT1) consists of at least three isozymes, namely, the hNMT1 long form ($hNMT1_L$), hNMT1 medium form ($hNMT1_M$), and hNMT1 short form ($hNMT1_S$); these isozymes were suggested to be produced by splice variants and to differ in translation start site [19,20]. Recently, it has been suggested that each

* Corresponding author. Tel.: +81 96 371 4362; fax: +81 96 362 7800.
E-mail address: shoji@gpo.kumamoto-u.ac.jp (S. Shoji).

1286-4579/$ - see front matter © 2007 Elsevier Masson SAS. All rights reserved.
doi:10.1016/j.micinf.2007.10.015

Please cite this article in press as: N. Takamune et al., HIV-1 production is specifically associated with human NMT1 long form in human NMT isozymes, Microb Infect (2007), doi:10.1016/j.micinf.2007.10.015

of the mouse NMT isozymes (mNMT1 and mNMT2) has different roles during mouse development [21]. However, it remains unclarified which isozyme catalyzes which substrate *in vivo*. Thus, it is important to understand which isozyme is closely associated with the HIV-1 life cycle, because the isozyme involved in HIV-1 replication could be used as a specific target in host factors for the development of anti-HIV-1 agents that are effective for evasive drug-resistant viruses. In this study, we tried to determine which hNMT isozyme plays a crucial role in HIV-1 production in which the *N*-myristoylation of $Pr55^{gag}$ is involved.

2. Materials and methods

2.1. Materials

HEK293 cells, infectious HIV-1 expression vectors pNL4-3, pYU-2, pYK-JRCSF, and p89.6 were obtained from the NIH AIDS Research & Reference Reagent Program. Dulbecco's modified Eagle's medium (DMEM) and RPMI 1640 medium were obtained from Nissui Pharmaceutical Co. Ltd.

2.2. Cell culture

HEK293 cells were cultured at 37 °C in DMEM supplemented with 10% heat-inactivated fetal calf serum containing 100 IU/ml penicillin and 100 μg/ml streptomycin in 5% CO_2

2.3. Double-stranded RNAs

The target sequences of double-stranded RNAs (dsRNAs) inducing RNAi against hNMT1 and hNMT2 were 5′-GCGAC CAATGGAAACAAAGGACATT-3′ and 5′-GCTCAAGGAG TTATACACGTTGTTA-3′, respectively. dsRNA with a nonspecific randomized sequence was used for the control experiments. dsRNAs were prepared as Stealth™ RNAi (Invitrogen, Carlsbad, CA).

2.4. Cell growth assay

HEK293 cells (4.0×10^4 cells) were cultured in 96-well plates overnight. The cells were transfected with 0, 3.1, 6.1, 12.5, 25, 50, and 100 pmol/ml siRNAs using Lipofectamine 2000 and cultured for 48 h. The cell viability was evaluated by WST-1 method [28]. The cell transfected with or without 10 pmol/ml of siRNAs were visually inspected by microscopy and photographed (×100).

2.5. Reverse transcription and semiquantitative real-time polymerase chain reaction (PCR)

Total RNA was extracted using ISOGEN (Nippon Gene Co. Ltd., Tokyo, Japan) according to the manufacturer's instruction. First-strand cDNA synthesis was performed using the SuperScript™ III First-Strand Synthesis System for RT–PCR (Invitrogen, Carlsbad, CA) according to the manufacturer's instruction, in which oligo $(dT)_{20}$ was used as a primer. DyNAmo™ HS SYBR®Green qPCR kit (Finnzymes, Espoo, Finland) reagents were used as semiquantitative real-time PCR reagents according to the manufacturer's instruction. Thermocycling was carried out using the DNA Engine Opticon®2 System (MJ Research Inc., Waltham, MA). The oligonucleotide primers used for the PCR were as follows: hNMT1 sense primer, CCGCAGATGATGGAAGGGAA; hNMT1 antisense primer, CCTCTCTGCTGGCAAAGAGTTCA; hNMT2 sense primer, GAAGTCCTGGAGGGTATTTG; hNMT2 antisense primer, CTGCATTGGAACACTGGGATT; β-actin sense primer, CGGAACCGCTCATTGCC; β-actin antisense primer, ACCCACATCGTGCCCATCTA.

2.6. Construction of each hNMT isozyme expression vector

Total RNA was extracted from CEM cells, a human T-cell line, using a QuickPrep Total RNA Extraction kit (Amersham Biosciences Corp, Piscataway, NJ) according to the manufacturer's instruction. First-strand cDNAs were obtained by the reverse transcription of total RNA using a Gene Amp RNA PCR kit (Applied Biosystems, Foster City, CA). The cDNA of each hNMT isozyme was amplified by PCR with *pfu* Turbo Hotstart DNA polymerase (Stratagene, La Jolla, CA) using a primer pair on the basis of the reported GenBank accession numbers: BC006569 for hNMT1 and AF043325 for hNMT2. The sequences of primers used for the construction of each hNMT isozyme expression vector in mammalian cells were as follows: CATGAATTCATGGCGGACGAGAGTGAGAC with the 5′-EcoRI restriction site for $hNMT1_L$ as the sense primer; CATGAATTCATGGAAGGGAACGGGAACGGC CATG with the 5′-EcoRI restriction site for $hNMT1_M$ as the sense primer; CATGAATTCATGAACTCTTTGCCAGCA GAG with the 5′-EcoRI restriction site for $hNMT1_S$ as the sense primer; CATCTCGAGTTATTGTAGCACCAGTC CAAC with the 5′-XhoI restriction site for all the hNMT1 isozymes as the antisense primer; CATGAATTCATGGCG GAGGACAGCGAGTC with the 5′-EcoRI restriction site for hNMT2 as the sense primer; and CATCTCGAGCTATTG TAGTACTAGTCCAAC with the 5′-XhoI restriction site for hNMT2 as the antisense primer. Each hNMT isozyme cDNA amplified by PCR was subcloned into the pT7Blue vector (Merck KGaA, Darmstadt, Germany) according to the manufacturer's instruction. Each cDNA digested with EcoRI and XhoI was cloned into the pcDNA4/HisMax vector (Invitrogen) for its expression in mammalian cells.

2.7. Site-directed mutagenesis for Gly^{412} to Lys^{412} mutation of each hNMT isozyme

The sequences of the primers used for the site-directed mutagenesis of each hNMT isozyme expression vector were as follows: CAGAGAAGGTTAAACTGGTGCTACAATAAC for the hNMT1 isozyme mutation sense primer; GTAGCAC CAGTTTAACCTTCTCTGCCCCC for the hNMT1 isozyme mutation antisense primer; CTGAAAAGGTTAAACTAG TACTACAATAG for the hNMT2 mutation sense primer; and

Please cite this article in press as: N. Takamune et al., HIV-1 production is specifically associated with human NMT1 long form in human NMT isozymes, Microb Infect (2007), doi:10.1016/j.micinf.2007.10.015

GTAGTACTAGTTTAACCTTTTCAGAATCTG for the hNMT2 mutation antisense primer. The mutations were induced using a QuikChange site-directed mutagenesis kit (Stratagene) according to the instruction manual.

2.8. Quantification of HIV-1 p24 antigen in supernatant

HEK293 cells (1.0×10^5 cells) were cultured in 48-well plates overnight. Confluent cells (30–50%) were cotransfected with 10 pmol of dsRNAs and HIV-1 expression vectors (pNL4-3, pYU-2, pYK-JRCSF, or p89.6) using Lipofectamine2000. Alternatively, HEK293 cells (3.0×10^5 cells) were cultured in 24-well plates overnight. The cells were transfected with a plasmid expressing each Xpress™ epitope-tagged hNMT isozyme ($hNMT1_L$, $hNMT1_M$, $hNMT1_S$, and hNMT2) or a comparable inactive form, whose plasmids are described in detail below, using Lipofectamine2000, and then transfected with pNL4-3 after 24 h. After 24 h or 48 h of further cultivation, the supernatant was collected and centrifuged to remove cell debris. The amount of HIV-1 p24 antigen in the cell-free supernatant was measured using an enzyme-linked immunosorbent assay (ELISA) kit (ZeptoMetrix Corp., Buffalo, NY) according to the manufacturer's instruction.

2.9. Cell lysis and Western immunoblot analysis

The cells were washed twice with phosphate-buffered saline, lysed in the lysis buffer, and subjected to sodium dodecyl sulfate–polyacrylamide gel electrophoresis (SDS–PAGE) and Western blot analysis [27]. The serum and antibodies used in different immunoblottings were as follows: HIV-1-positive plasma (a gift from Dr. Shuzo Matsushita of Kumamoto University, AIDS Research Institute, Kumamoto, Japan), actin (Ab-1) kit (Oncogene Research Products, Boston, MA), anti-Xpress™ antibody (Invitrogen), anti-caveolin-1 (Sigma, St. Louis, MO), anti-transferrin receptor (BD Pharmingen, San Diego, CA), anti-NMT1 (BD Pharmingen), and anti-NMT2 (BD Pharmingen). Immune complexes were detected with appropriate peroxidase-conjugated secondary antibodies followed by visualization by chemiluminescence detection (NEN Life Science Products, Boston, MA).

2.10. Flotation assay and Western blot analysis

Flotation assay was performed as previously described [22]. The final five fractions were prepared from the top to the bottom of the tube and subjected to SDS–PAGE and Western immunoblot analysis as described above. HIV-1 antigens were probed with HIV-1-positive plasma. The transferrin receptor and caveolin-1 were used as non-DRM and DRM markers, respectively.

3. Results

3.1. Inhibition of expressions of hNMT1 isozymes and hNMT2 by RNAi

There are two kinds of mRNA, namely, extended 5′-mRNA and alternatively spliced mRNA, in hNMT1, from which $hNMT1_L$, $hNMT1_M$, and $hNMT1_S$ could be produced [20]; however, the *hNMT2* gene produces only one protein: hNMT2 [17]. In this study, two kinds of chemically synthetic double-stranded siRNA were designed: one targets all kinds of hNMT1 mRNA and the other targets hNMT2 mRNA. siRNA with a randomized sequence was also used for the control experiments. HEK293 cells were transfected with siRNAs and cultured for 48 h. The effects of the siRNAs at doses from 0 to 100 pmol/ml on cell growth were evaluated by the WST-1 method. As shown in Fig. 1A, similar dose-dependent cytotoxic effect of siRNAs was observed in the three siRNAs. The treatment of HEK293 cells with 10 pmol/ml siRNAs, which show no cytotoxic effect, showed no change in cell morphology compared with the nontreatment of HEK293 cells (Fig. 1B). the siRNA dose of 10 pmol/ml was therefore used for the other subsequent experiments. To examine whether siRNAs knock down mRNAs specifically, HEK293 cells were transfected with siRNAs and cultured for 48 h. mRNA level was semiquantified by real-time RT–PCR analysis. β-Actin mRNA was selected as the internal standard for semiquantification. The hNMT1 and hNMT2 mRNA expression levels of HEK293 cells treated with each siRNA decreased from about 20% to 30% the expression level of each control mRNA (Fig. 1C and D, respectively). Additionally, the each specific suppression of isozyme by each siRNA was observed (Fig. 1C and D).

3.2. Failure of specific localization of $Pr55^{gag}$ in DRM with knockdown of hNMT1 isozymes

$Pr55^{gag}$ is associated with the DRM fraction during assembly in the late stage of HIV-1 replication [13,14], in which its localization is dependent on its *N*-myristoylation [13]. The effect of the knockdown of each NMT isozyme on the localization of $Pr55^{gag}$ in the DRM fraction was therefore evaluated. pNL4-3-transfected HEK293 cells were treated with siRNA directed by either hNMT1 or hNMT2, cultured and subjected to flotation assay [22]. The pNL4-3G2A mutant was used in addition to wild-type pNL4-3 in the control experiment for comparison of the localizations of non-*N*-myristoylated $Pr55^{gag}$ and *N*-myristoylated $Pr55^{gag}$. The transferrin receptor and caveolin-1 were used as the non-DRM and DRM markers, respectively. As shown in Fig. 2*N*-myristoylated $Pr55^{gag}$ in pNL4-3-transfected HEK293 cells was specifically detected in fraction 1 similarly to caveolin-1, defined as the DRM fraction, whereas a large amount of non-*N*-myristoylated $Pr55^{gag}$ in pNL4-3G2A-mutant-transfected HEK293 cells was detected, as expected, in the fraction similar to that for the transferrin receptor, defined as the non-DRM fraction. These results show that the specific localization of $Pr55^{gag}$ in DRM is

Please cite this article in press as: N. Takamune et al., HIV-1 production is specifically associated with human NMT1 long form in human NMT isozymes, Microb Infect (2007), doi:10.1016/j.micinf.2007.10.015

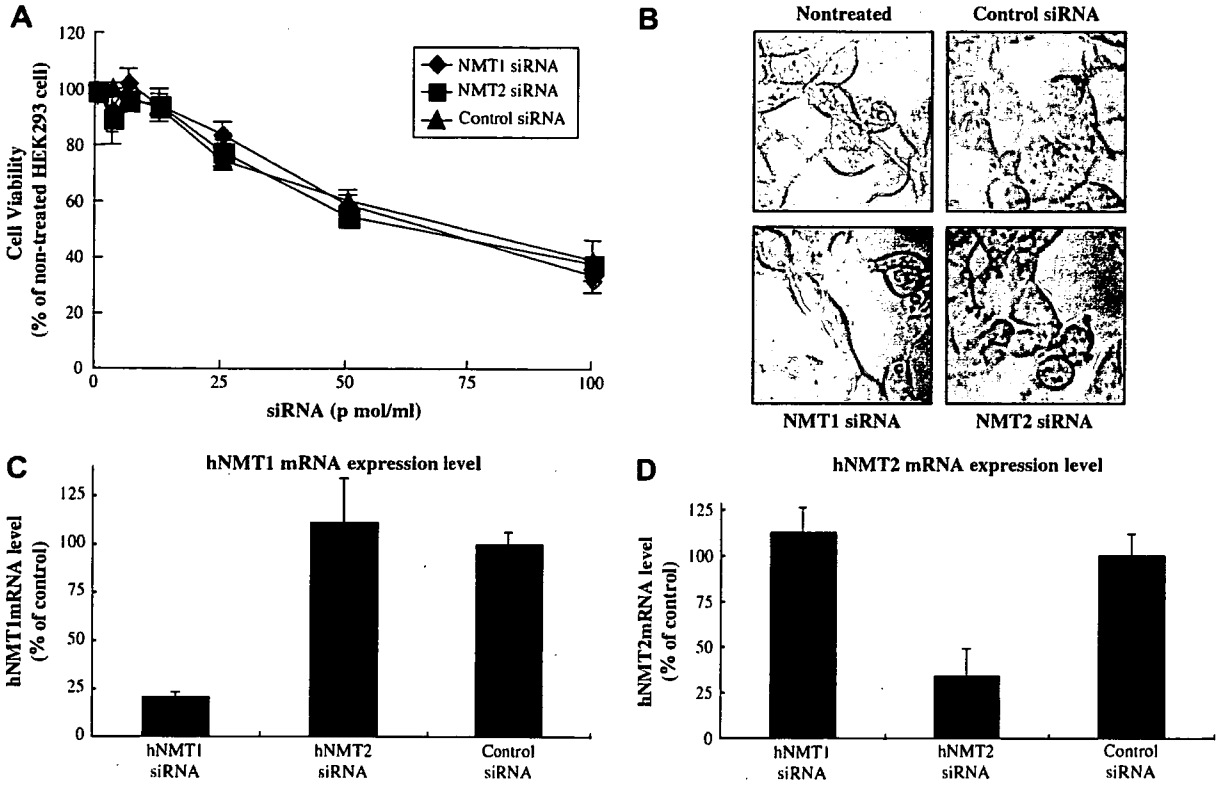

Fig. 1. Inhibition of hNMT1 and hNMT2 mRNA expressions by siRNAs in HEK293 cells. HEK293 cells were transfected with hNMT1- and hNMT2-specific siRNAs and control siRNA separately. The cells were harvested at 48 h post-transfection. The dose-dependent effect of siRNAs on cell growth was evaluated by the WST-1 method as described in Materials and methods (A). The cell morphology 48 h after transfection of each siRNA (10 pmol/ml) was visually inspected by microscopy and photographed (×100) (B). The mRNA expression levels of hNMT1 (C) and hNMT2 (D) were semiquantified by real-time PCR analysis using specific primer pairs, as described in Section 2. β-Actin mRNA level was used as the internal standard. Cell viability and mRNA expression level are expressed as percentage relative to those obtained in the siRNA-nontreated and control siRNA-treated experiments, respectively. Means and standard deviations from three independent experiments are shown.

dependent on *N*-myristoylation, as previously demonstrated [13]. By performing the same flotation assay, the localization of $Pr55^{gag}$ was examined in HEK293 cells with all the hNMT1 isozymes or hNMT2 knocked down. As shown in Fig. 2, $Pr55^{gag}$ was detected in the non-DRM fraction from the HEK293 cells with all the hNMT1 isozymes knocked down. On the other hand, $Pr55^{gag}$ was specifically detected in the DRM fraction from the HEK293 cells with hNMT2 knocked down, similarly to that observed in the control experiment.

3.3. Knockdown of hNMT1 isozymes affects HIV-1 release

Since $Pr55^{gag}$ *N*-myristoylation appears to be required in the release of HIV-1 particles [11,12], the late stage of the HIV-1 life cycle must be directly involved in either or both hNMT isozymes. As control experiment, a comparison of HIV-1 production between pNL4-3 and pNL4-3G2A mutant was conducted in parallel. The production of HIV-1 with non-*N*-myristoylated $Pr55^{gag}$ was about 13% that of the wild-type HIV-1 (Fig. 3E); however, the expression levels of $Pr55^{gag}$ in HEK293 cells, which were confirmed by Western immunoblot analysis, were almost the same between the wild-type HIV-1 and the mutant HIV-1 (Fig. 3E).

The effects of siRNAs on the production of the HIV-1 progeny were evaluated, in which HEK293 cells transfected with infectious HIV-1 expression vectors, namely, pNL4-3, p89.6, pYK-JRCSF, and pYU2, were used. The amount of HIV-1 p24 antigen in the supernatant was quantified by ELISA to evaluate HIV-1 production. As shown in Fig. 3A–D, the amount of HIV-1 p24 antigen in the supernatant of cells with the hNMT1 isozymes knocked down was significantly lower than that in the supernatant of the control cells for all the HIV-1 strains tested, whereas the amount of HIV-1 p24 antigen in the supernatant of the cells with hNMT2 knocked down was the same as that in the supernatant of the control cells for all the HIV-1 strains tested. The significant reduction in HIV-1 production was dependent on the knockdown of the hNMT1 isozymes. The knockdown of the hNMT1 isozymes was sufficient to significantly decrease HIV-1 production in the experiments. Similar expression levels of $Pr55^{gag}$ as an expression product of the HIV-1 gene in the transfected cells (Fig. 3A–E), in which actin was detected as internal control, were confirmed. Taken together, the results indicate that

Please cite this article in press as: N. Takamune et al., HIV-1 production is specifically associated with human NMT1 long form in human NMT isozymes, Microb Infect (2007), doi:10.1016/j.micinf.2007.10.015

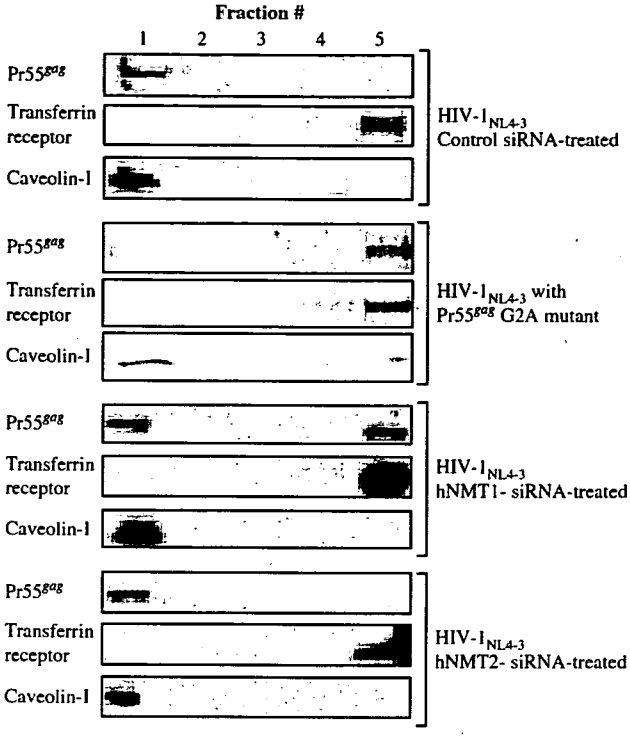

Fig. 2. Effect of knockdown of either hNMT1 or hNMT2 on localization of $Pr55^{gag}$ in DRM and non-DRM fractions. HEK293 cells were transfected with siRNA against hNMT1, hNMT2 and control as indicated at 48 h post-transfection with pNL4-3. The cells 96 h after the initial transfection were washed and subjected to flotation assay. The pNL4-3G2A mutant was used to detect the localization of non-*N*-myristoylated $Pr55^{gag}$ as the control experiment. Results of experiments involving treatment with each siRNA are shown. $Pr55^{gag}$ was detected by Western immunoblot analysis using HIV-1-positive plasma. The transferrin receptor and caveolin-1 were used as the non-DRM and DRM markers, respectively.

hNMT1 contributes to HIV-1 production more than hNMT2 in the late stage of HIV-1 replication.

3.4. Coexpression of inactive hNMT1$_L$ mutant with HIV-1 decreases HIV-1 production

As shown in Figs. 2 and 3, the results of the experiments with siRNAs strongly suggest that hNMT1 isozymes are involved in the late stage of HIV-1 replication. To determine which hNMT1 isozyme (hNMT1$_L$, hNMT1$_M$, or hNMT1$_S$) most effectively contributes to HIV-1 production, inactive mutants of the hNMT1 isozymes were used as dominant negative mutants for the evaluation. The inactive form of hNMT2 was also used as the negative control, because the knockdown experiments with hNMT2 siRNA showed no inhibitory effect on HIV-1 production (Fig. 3). Each Xpress epitope-tagged hNMT isozyme expression vector was constructed, and site-directed mutation for Gly^{412} to Lys^{412} in all the hNMT1 isozymes and hNMT2 was introduced in Section 2, in which the number corresponds to hNMT1$_S$ and the amino acid is located five residues from the *C*-terminus of each isozyme. It was previously reported that comparable mutants are inactive forms of human and yeast NMTs [16]. Each of the wild-type and mutant hNMT isozymes was separately expressed in HEK293 cells by each Xpress epitope-tagged expression vector, followed by transfection with pNL4-3. The amounts of HIV-1 p24 antigen in the supernatant 24 h and 48 h after pNL4-3 transfection were quantified by ELISA to evaluate HIV-1 production. As shown in Fig. 4A–C, the amounts of HIV-1 p24 antigen in the supernatants of hNMT1$_L$-mutant-expressing HEK293 cells 24 h and 48 h after the transfection were significantly lower than that in the supernatant of wild-type-hNMT1$_L$-expressing HEK293 cells (Fig. 4C). On the other hand, no differences between the wild type and the mutant were observed for the other hNMT1 isozymes (Fig. 4A,B). As expected, no effect of the inactive form of hNMT2 on HIV-1 production was observed (Fig. 4D). Similarities in expression level between the wild types and the mutants were observed for the respective sets of Xpress-tagged NMT isozymes studied (Fig. 4E–G). Similar expression levels of $Pr55^{gag}$ in each of the transfected cells were also observed (Fig. 4E–G). Actin was used as internal control in each sample.

As shown in Fig. 4I, endogenous NMT1 and NMT2 isozymes were detected by Western immunoblot analysis. As shown in Fig. 4I, a higher expression level of endogenous NMT1$_L$ than of other NMT1 isozymes was observed, in which endogenous NMT1$_M$ and NMT1$_S$ expressed about 30% and 15% that of NMT1$_L$, respectively.

4. Discussion

N-Myristoylation is acylation specific to N-terminal Gly in proteins, which is an important component of membrane-targeting signals in general. Many kinds of viral protein are *N*-myristoylated [6], for example, the VP4 of the poliovirus [23], the VP2 of the simian virus 40 [24], the L protein of the hepatitis B virus [25], and the $pp60^{src}$ of the Rous sarcoma virus [26] in addition to the $Pr55^{gag}$ and Nef of HIV-1. Since NMT is a common host factor for many kinds of virus, it is important to understand the detailed relationship between NMT and the replication of each virus. In this study, we focus on the relationship between HIV-1 production and each hNMT isozyme.

We hypothesize that each hNMT isozyme exclusively or predominantly catalyzes the *N*-myristoylation of specific substrate proteins *in vivo* or that each hNMT isozyme has a specific role *in vivo*. For example, $Pr55^{gag}$ could be *N*-myristoylated with a specific hNMT isozyme.

$Pr55^{gag}$ *N*-myristoylation is closely associated with HIV-1 phenotypes including the $Pr55^{gag}$ localization to the DRM fraction [13,14] and HIV-1 production [11]. $Pr55^{gag}$ *N*-myristoylation can efficiently drive $Pr55^{gag}$ to the cell membrane after translation [27] and enhance the association of $Pr55^{gag}$ with DRM [13], followed by the assembly of $Pr55^{gag}$ and the budding of viral particles [14]. The late stage of HIV-1 replication was therefore focused on to evaluate the contribution of each isozyme to the HIV-1 life cycle.

In the flotation assay, the localization of $Pr55^{gag}$ in the non-DRM fraction was observed with the knockdown of the

Please cite this article in press as: N. Takamune et al., HIV-1 production is specifically associated with human NMT1 long form in human NMT isozymes, Microb Infect (2007), doi:10.1016/j.micinf.2007.10.015

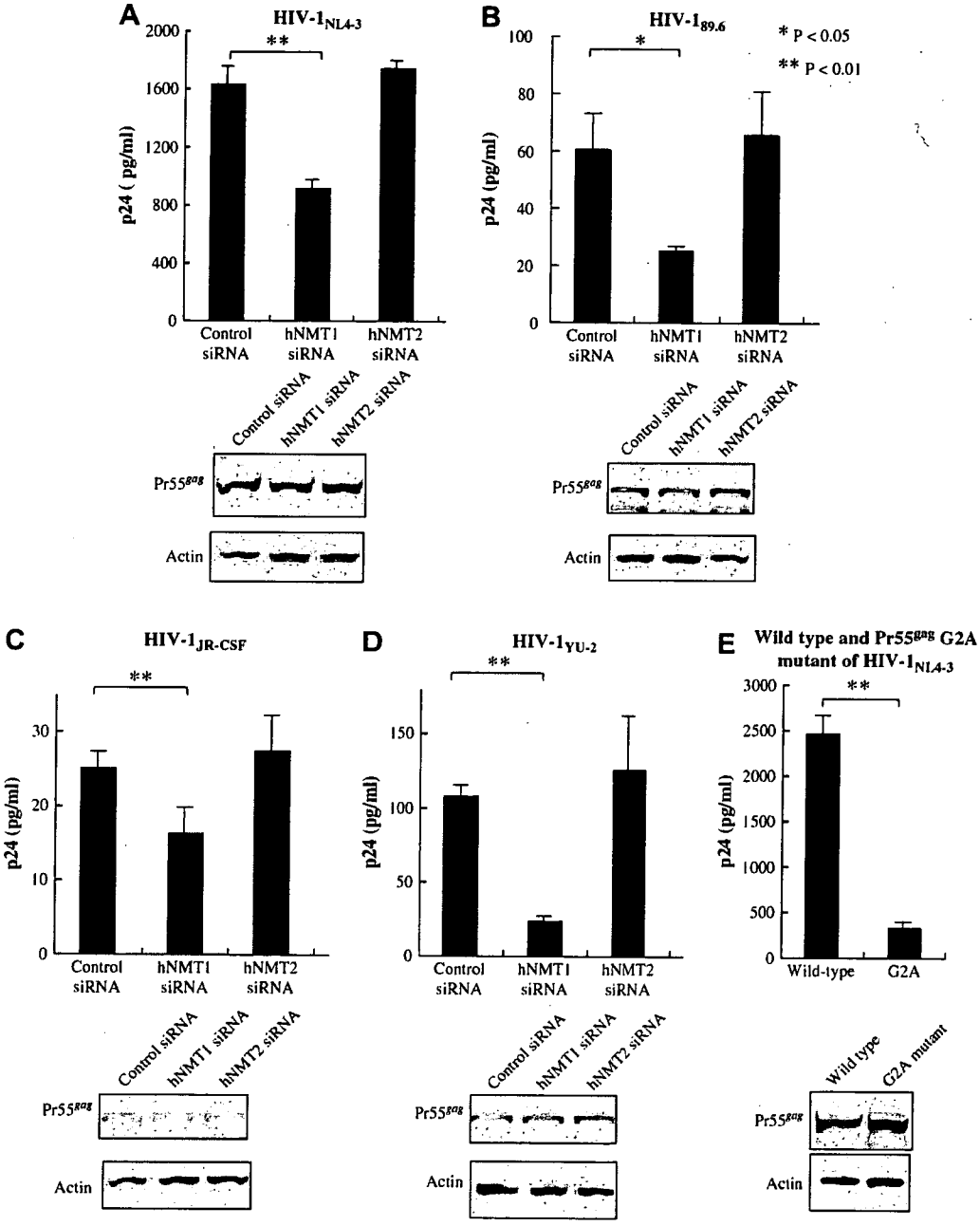

Fig. 3. Effect of knockdown of hNMT isozymes on HIV-1 production. HEK293 cells were cotransfected with siRNA and an HIV-1 expression vector. Alternatively, HEK293 cells were transfected with pNL4-3 or the pNL4-3G2A mutant. The amount of HIV-1 p24 antigen in the supernatant at 48 h post-transfection was quantified by ELISA, as described in Section 2. Each cell lysate was analyzed by Western immunoblot analysis, as described in Section 2. The expressions of $Pr55^{gag}$ as an expression product of the HIV-1 gene and actin as internal control are shown in the upper and bottom panels, respectively. (A) pNL4-3 (B) p89.6, (C) pYK-JRCSF, (D) pYU-2, (E) pNL4-3 and pNL4-3 G2A mutant. Means and standard deviations from three independent experiments are shown. *P* was calculated using Student's *t*-test. $*P < 0.05$ and $**P < 0.01$ for control siRNA vs. either hNMT1 siRNA.

hNMT1 isozymes except hNMT2 (Fig. 2). It was also shown that the significant reduction in HIV-1 production is dependent on the knockdown of the hNMT1 isozymes in all the HIV-1 strains tested (Fig. 3A–D). The results suggest that a large amount of non-*N*-myristoylated $Pr55^{gag}$ with the knockdown of all the hNMT1 isozymes but not hNMT2 localizes in the non-DRM fraction, in which no appropriate $Pr55^{gag}$ assembly occurs, resulting in a decreased HIV-1 production.

Overall, the reduction rate of the p24 antigen of each viral strain in the supernatant by hNMT1 siRNA (Fig. 3) was less than that of hNMT mRNA by hNMT1 siRNA (Fig. 1C). These results seem reasonable, because even if $Pr55^{gag}$ was not *N*-myristoylated by

Please cite this article in press as: N. Takamune et al., HIV-1 production is specifically associated with human NMT1 long form in human NMT isozymes, Microb Infect (2007), doi:10.1016/j.micinf.2007.10.015

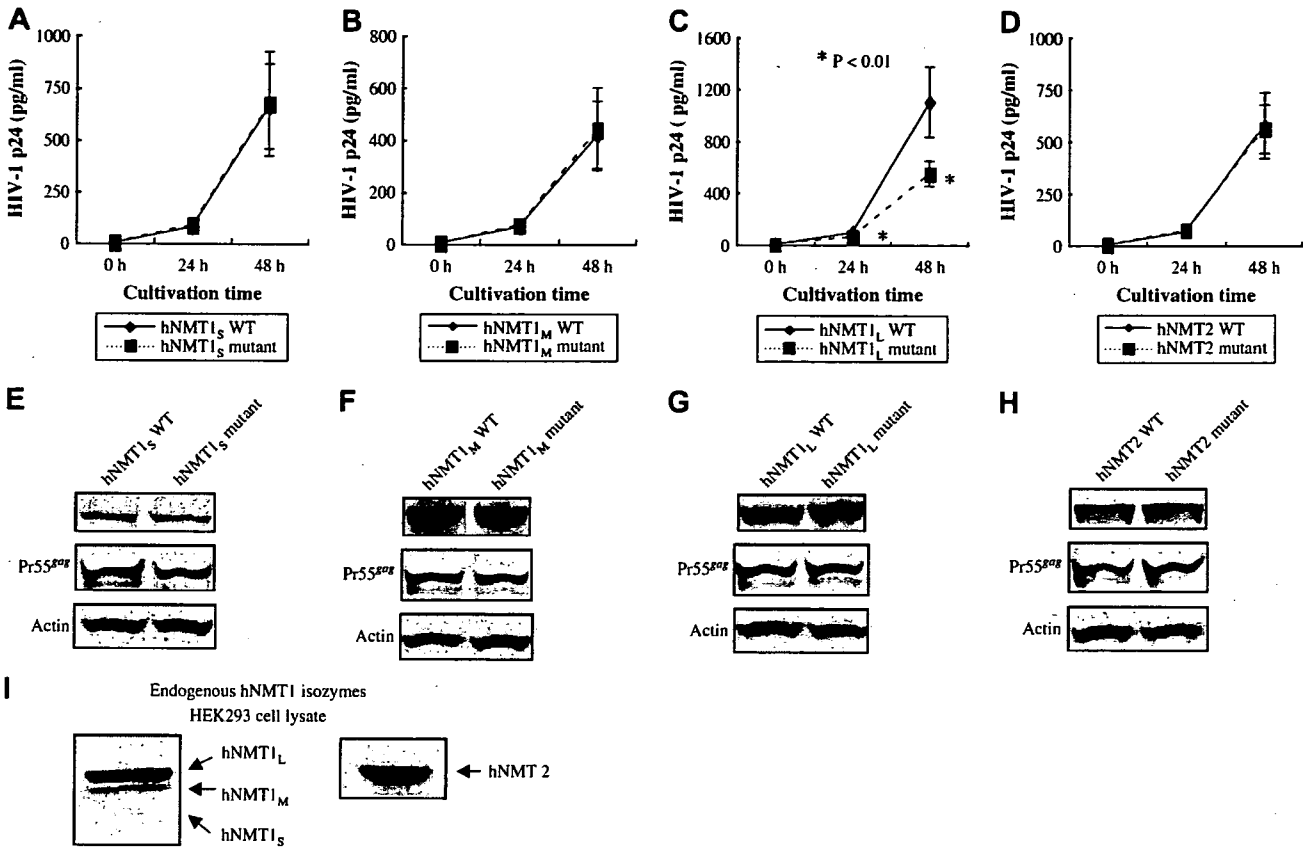

Fig. 4. Effect of each inactive hNMT isozyme mutant on HIV-1 production. HEK293 cells were transfected with a plasmid expressing each Xpress™ epitope-tagged hNMT isozyme ($hNMT1_L$, $hNMT1_M$, $hNMT1_S$, and hNMT2) or a comparable inactive form, followed by transfection with pNL4-3 after 24 h. The amount of HIV-1 p24 antigen in the supernatant 24 h and 48 h after transfection with pNL4-3 was quantified by ELISA, as described in Section 2 (A–D). Each cell lysate 48 h after transfection was analyzed by Western immunoblot analysis, as described in Section 2. The expressions of each Xpress-tagged NMT isozyme, $Pr55^{gag}$ as an expression product of the HIV-1 gene, and actin as internal control are shown in the upper, middle, and bottom panels, respectively (E–H). Nontreated HEK293 cell lysate was subjected to SDS–PAGE and Western immunoblot analysis to detect endogenous NMT1 and NMT2 using anti-NMT1 and anti-NMT2, respectively, as described in Section 2 (I). Means and standard deviations from four independent experiments are shown for the ELISA results. *P* was calculated using Student's *t*-test. $^*P < 0.01$ for active form vs. comparable inactive form after 24 h or 48 h of cultivation.

the G2A mutation of the amino terminus, the reduction rate of the p24 antigen was not 100% but about 90% (Fig. 3E).

The evaluation of the dominant negative effect exerted by the inactive form of each hNMT1 isozyme on HIV-1 production resulted in a significant reduction in HIV-1 production by the $hNMT1_L$ mutant (Fig. 4C). It is thought that the mutant $hNMT1_L$ partly competed with endogenous $hNMT1_L$ for substrate proteins including $Pr55^{gag}$, whereas the mutants of $hNMT1_S$, $hNMT1_M$, and hNMT2 competed with their corresponding endogenous forms for substrate proteins excluding $Pr55^{gag}$.

Since a higher expression level of endogenous $hNMT1_L$ than of other hNMT1 isozymes was observed in HEK293 cells (Fig. 4I), the dominant negative effect of the mutant seems to attenuate. Additionally, the difference in viral production between the coexpression of wild-type $hNMT1_L$ and that of the mutant might have resulted from the sum of the suppression of HIV-1 production by the mutant and the enhancement of HIV-1 production by the wild-type $hNMT1_L$.

It should be considered that $hNMT1_L$ disruption could affect not only the $Pr55^{gag}$ function but also the functions of some cellular substrate proteins, which could lead to the inhibition of HIV-1 production. Although it is extremely difficult to comprehensively understand at this point which substrate proteins of $hNMT1_L$ are involved *in vivo*, at least $Pr55^{gag}$ is the likely substrate of $hNMT1_L$ *in vivo*. At the same time, it could be expected that $hNMT1_L$ disruption could not affect the functions of substrate proteins associated with $hNMT1_S$, $hNMT1_M$, and hNMT2 *in vivo*.

Interestingly, it appeared that recombinant hNMT1 and hNMT2 could catalyze the *N*-myristoylation of peptide substrates derived from $Pr55^{gag}$ according to the results of the *in vitro* experiments (data not shown). It is therefore suggested that the affinity between hNMT1 and the N-terminal amino acid sequence of $Pr55^{gag}$ is not the only determinant for the exclusive hNMT1 utilization by $Pr55^{gag}$ *in vivo*.

Altogether, the results suggest that $hNMT1_L$ is specifically associated with the late stage of HIV-1 replication *in vivo*. The contribution of our study to progress in this research area is the clarification of the hNMT isozyme that could be a more specific target molecule for the development of anti-HIV-1 agents

Please cite this article in press as: N. Takamune et al., HIV-1 production is specifically associated with human NMT1 long form in human NMT isozymes, Microb Infect (2007), doi:10.1016/j.micinf.2007.10.015

that could inhibit the DRM localization of $Pr55^{gag}$. Additionally, results of our study suggest that each hNMT isozyme has a specific role *in vivo*, from which an interesting question arises: "What is the mechanism underlying the specific role of each hNMT isozyme *in vivo*?" Answers to this question and others are expected to contribute to the development of not only novel anti-HIV strategies but also strategies against other pathogenic viruses with *N*-myristoylation.

Acknowledgments

We thank Dr. S. Matsushita (Kumamoto University, AIDS Research Institute, Kumamoto, Japan) for providing the HIV-1-positive plasma. This study was supported in part by a Grant-in-Aid for Scientific Research from the Ministry of Education, Culture, Sports, Science and Technology of Japan, and a Health Science Research Grant from the Ministry of Health, Labour, and Welfare of Japan.

References

[1] D.A. Towler, S.P. Adams, S.R. Eubanks, D.S. Towery, E. Jackson-Machelski, L. Glaser, J.I. Gordon, Myristoyl CoA:protein N-myristoyltransferase activities from rat liver and yeast possess overlapping yet distinct peptide substrate specificities, J. Biol. Chem. 263 (1988) 1784–1790.

[2] D.A. Towler, L. Glaser, Protein fatty acid acylation: enzymatic synthesis of an N-myristoylglycyl peptide, Proc. Natl. Acad. Sci. U.S.A. 83 (1986) 2812–2816.

[3] J. Zha, S. Weiler, K.J. Oh, M.C. Wei, S.J. Korsmeyer, Posttranslational N-Myristoylation of BID as a molecular switch for targeting mitochondria and apoptosis, Science 290 (2000) 1761–1765.

[4] S.A. Carr, K. Biemann, S. Shoji, D.C. Parmelee, K. Titani, n-Tetradecanoyl is the NH2-terminal blocking group of the catalytic subunit of cyclic AMP-dependent protein kinase from bovine cardiac muscle, Proc. Natl. Acad. Sci. U.S.A. 79 (1982) 6128–6131.

[5] M.D. Resh, Fatty acylation of proteins: new insights into membrane targeting of myristoylated and palmitoylated proteins, Biochim. Biophys. Acta. 1451 (1999) 1–16.

[6] J.A. Boutin, Myristoylation, Cell Signal 9 (1997) 15–35.

[7] R.J. Mervis, N. Ahmad, E.P. Lillehoj, M.G. Raum, F.H. Salazar, H.W. Chan, S. Venkatesan, The gag gene products of human immunodeficiency virus type 1: alignment within the gag open reading frame, identification of posttranslational modifications, and evidence for alternative gag precursors, J. Virol. 62 (1988) 3993–4002.

[8] S. Shoji, A. Tashiro, Y. Kubota, Antimyristoylation of gag proteins in human T-cell leukemia and human immunodeficiency viruses with N-myristoyl glycinal diethylacetal, J. Biochem. 103 (1988) 747–749.

[9] F.D. Veronese, T.D. Copeland, S. Oroszlan, R.C. Gallo, M.G. Samgadharan, Biochemical and immunological analysis of human immunodeficiency virus gag gene products p17 and p24, J. Virol. 62 (1988) 795–801.

[10] B. Guy, M.P. Kieny, Y. Riviere, C. Le Peuch, K. Dott, M. Girard, L. Montagnier, J.P. Lecocq, HIV F/3′ orf encodes a phosphorylated GTP-binding protein resembling an oncogene product, Nature 330 (1987) 266–269.

[11] M. Bryant, L. Ratner, Myristoylation-dependent replication and assembly of human immunodeficiency virus 1, Proc. Natl. Acad. Sci. U.S.A. 87 (1990) 523–527.

[12] K.H. Furuishi, M. MatsuokaTakama, I. Takahashi, S. Misumi, S. Shoji, Blockage of N-myristoylation of HIV-1 gag induces the production of impotent progeny virus, Biochem. Biophys. Res. Commun. 237 (1997) 504–511.

[13] L. Ding, A. Derdowski, J.-J. Wang, P. Spearman, Independent segregation of human immunodeficiency virus type 1 Gag protein complexes and lipid rafts, J. Virol. 77 (2003) 1916–1926.

[14] A. Ono, E.O. Freed, Plasma membrane rafts play a critical role in HIV-1 assembly and release, Proc. Natl. Acad. Sci. U.S.A. 98 (2001) 13925–13930.

[15] A. Tashiro, S. Shoji, Y. Kubota, Antimyristoylation of the gag proteins in the human immunodeficiency virus-infected cells with N-myristoyl glycinal diethylacetal resulted in inhibition of virus production, Biochem. Biophys. Res. Commun. 165 (1989) 1145–1154.

[16] R.J. Duronio, S.I. Reed, J.I. Gordon, Mutations of human myristoyl-CoA:protein N-myristoyltransferase cause temperature-sensitive myristic acid auxotrophy in Saccharomyces cerevisiae, Proc. Natl. Acad. Sci. U.S.A. 89 (1992) 4129–4133.

[17] D.K. Giang, B.F. Cravatt, A second mammalian N-myristoyltransferase, J. Biol. Chem. 273 (1998) 6595–6598.

[18] V. Rioux, E. Beauchamp, F. Pedrono, S. Daval, D. Molle, D. Catheline, P. Legrand, Identification and characterization of recombinant and native rat myristoyl-CoA:protein N-myristoyltransferases, Mol. Cell Biochem. 286 (2006) 161–170.

[19] C.J. Glover, K.D. Hartman, R.L. Felsted, Human N-myristoyltransferase amino-terminal domain involved in targeting the enzyme to the ribosomal subcellular fraction, J. Biol. Chem. 272 (1997) 28680–28689.

[20] R.A. McIlhinney, K. Young, M. Egerton, R. Camble, A. White, M. Soloviev, Characterization of human and rat brain myristoyl-CoA: protein N-myristoyltransferase: evidence for an alternative splice variant of the enzyme, Biochem. J. 333 (1998) 491–495.

[21] S.H. Yang, A. Shrivastav, C. Kosinski, R.K. Sharma, M.H. Chen, L.G. Berthiaume, L.L. Peters, P.T. Chuang, S.G. Young, M.O. Bergo, N-Myristoyltransferase 1 is essential in early mouse development, J. Biol. Chem. 282 (2005) 18990–18995.

[22] S. Manes, E. Mira, C. Gomez-Mouton, R.A. Lacalle, P. Keller, J.P. Labrador, C. Martinez-A, Membrane raft microdomains mediate front-rear polarity in migrating cells, EMBO J. 18 (1999) 6211–6220.

[23] A.V. Paul, A. Schultz, S.E. Pincus, S. Oroszlan, E. Wimmer, Capsid protein VP4 of poliovirus is *N*-myristoylated, Proc. Natl. Acad. Sci. U.S.A. 84 (1999) 7827–7831.

[24] C.H. Streuli, B.E. Griffin, Myristic acid is coupled to a structural protein of polyoma virus and SV40, Nature 326 (1987) 619–622.

[25] P. Gripon, J. Le Seyec, S. Rumin, C. Guguen-Guillouzo, Myristoylation of the hepatitis B virus large surface protein is essential for viral infectivity, Virology 213 (1995) 292–299.

[26] A.M. Schultz, L.E. Henderson, S. Oroszlan, E.A. Garber, H. Hanafusa, Amino terminal myristoylation of the protein kinase p60src, a retroviral transforming protein, Science 227 (1985) 427–429.

[27] T. Shiraishi, S. Misumi, M. Takama, I. Takahashi, S. Shoji, Myristoylation of human immunodeficiency virus type 1 gag protein is required for efficient env protein transportation to the surface of cells, Biochem. Biophys. Res. Commun. 282 (2001) 1201–1205.

[28] M. Ishiyama, M. Shiga, K. Sakamoto, M. Mizoguchi, P.-G. He, A new sulfonated tetrazolium salt that produces a highly water-soluble formazan dye, Chem. Pharm. Bull. 41 (1993) 1118–1122.

Please cite this article in press as: N. Takamune et al., HIV-1 production is specifically associated with human NMT1 long form in human NMT isozymes, Microb Infect (2007), doi:10.1016/j.micinf.2007.10.015

Immunoreactive Cycloimmunogen Design Based on Conformational Epitopes Derived from Human Immunodeficiency Virus Type 1 Coreceptors: Cyclic Dodecapeptides Mimic Undecapeptidyl Arches of Extracellular Loop-2 in Chemokine Receptor and Inhibit Human Immunodeficiency Virus Type 1 Infection

Shogo Misumi, Nobutoki Takamune and Shozo Shoji*

Department of Pharmaceutical Biochemistry, Faculty of Medical and Pharmaceutical Sciences, Kumamoto University, Kumamoto 862-0973, Japan

Abstract: Human immunodeficiency virus type 1 (HIV-1) requires a chemokine receptor (CCR5 or CXCR4) as a coreceptor not only for initiate viral entry but also protecting highly conserved neutralization epitopes from the attack of neutralizing antibodies. Over the past decade, many studies have provided new insights into the HIV entry mechanism and have focused on developing an effective vaccine strategy. However, to date, no vaccine that can provide protection from HIV-1 infection has been developed. One reason for the disappointing results has been the inability of current vaccine candidates to elicit a broadly reactive immunity to viral proteins such as the envelope (env) protein. Here, we propose that chemokine receptors are attractive targets of vaccine development because their structures are highly conserved and that our synthetic cycloimmunogens can mimic conformational-specific epitopes of undecapeptidyl arches (UPAs: R_{168}-C_{178} in CCR5, N_{176}-C_{186} in CXCR4) and be useful for HIV-1 novel vaccine development.

Key Words: Cycloimmunogen, HIV-1, conformational epitope, CCR5, CXCR4.

INTRODUCTION

Two decades of intensive research has clarified the acquired immune deficiency syndrome (AIDS) causative agent, HIV-1, and many valuable details about the host-pathogen relationship. At the end of 1995, Cocchi *et al.* indicated that CC-chemokines, CCL3, CCL4, and CCL5, could inhibit HIV-1 replication [1]. Furthermore, at the beginning of 1996, Feng *et al.* showed that a second HIV-1 coreceptor beside CD4 was shown to be a chemokine receptor CXCR4 [2]. These independent discoveries opened a new frontier in HIV-1 research. Immediately after these discoveries it was shown that the counterpart of CXCR4 for strains associated with acute infection is the CC-chemokine receptor CCR5 [3-7]; a 32-bp deletion within the coding sequence of the CCR5 gene (CCR5-dela32) was found to be strongly protective against HIV-1 infection *in vitro* and *in vivo* [8-10]; and CXCL12 was identified as a specific CXCR4 ligand [11, 12]. These discoveries have greatly advanced our knowledge of the virus and the pathogenesis of HIV-1 infection for the development of novel therapeutic agents such as entry inhibitors and vaccines targeting the HIV-1 env protein. However, to date, there have been no antiretroviral therapies that can effectively eradicate HIV-1 infection *in vivo*.

Several studies have shown that a small number of HIV-exposed individuals do not become infected or can control HIV-1 infection at levels below the detection limit of standard assays, despite repeated and long-term exposures to the virus [13]. These individuals are defined as exposed seronegative (ESN). Although many different factors (e.g., CC-chemokine and neutralizing antibody (Ab) level) have been considered to explain the long-lasting protection in ESN individuals [13], we focused on the protective effects of anti-CCR5 autoantibodies in ESN individuals because these individuals possessing the delta32-CCR5 allele are healthy and highly resistant to HIV-1 infection [8-10, 14-17]. Therefore, to reproduce the ESN status with a candidate vaccine, chemokine receptors are attractive targets because they are cellularly highly conserved structures, unlike the HIV-1 env protein, that may rapidly mutate during the disease progression, and are the inescapable gateway for HIV-1 *in vivo*.

In this review article, we will introduce the findings on the immunogenicity of the cycloimmunogen mimicking the HIV-1 coreceptor CCR5 or CXCR4 and anti-HIV activities of induced Abs and antisera in mice and cynomolgus macaques.

DESIGN OF CHEMOKINE RECEPTOR-BASED HIV-1 VACCINE

Basic Mechanism of HIV-1 Entry

The HIV-1 mature envelope glycoprotein complex plays a pivotal role in the early events of viral attachment and entry into a target cell. The complex is arranged in a trimeric configuration of heterodimers, each consisting of a gp120 subunit noncovalently associated with a gp41 subunit after gp160 polypeptide chains are cleaved into two fragments, gp120 and gp41 [18-20]. The cleavage enables these proteins to undergo the first conformational changes before a virus interacts with CD4, and its coreceptor, CCR5 or CXCR4 [2, 21-23]. Furthermore, the second conformational changes are induced by CD4 binding and are required for the subsequent interaction between gp120 and its coreceptor. For binding to

*Address correspondence to this author at the Department of Pharmaceutical Biochemistry, Faculty of Medical and Pharmaceutical Sciences, Kumamoto University, 5-1 Oe-Honmachi, Kumamoto 862-0973, Japan; Tel: 81-96-371-4363; Fax: 81-96-362-7800; E-mail: shoji@gpo.kumamoto-u.ac.jp

1871-5303/07 $50.00+.00

a coreceptor, the third variable (V3) domain of gp120 was identified as an important determinant, which makes direct interaction with a coreceptor [1, 4]. Generally, the structure and charge of the V3 loop change the specificity of coreceptor use. The bridging sheet was also identified as another important determinant, which mainly recognizes the chemokine receptor [24]. Finally, gp41 undergoes additional conformational changes resulting in the fusion of the viral and target cell membranes. [25, 26]. Therefore, the important extracellular domains of a coreceptor that the V3 domain and bridging sheet interact with are attractive targets for developing an HIV-1 entry inhibitor.

Functional Determinants of CCR5 for HIV-1 Entry

A lot of mutation and chimeric studies of HIV-1 coreceptors have provided important information on the extracellular domain involved in the interaction with gp120. Although the gp120-binding domain of an HIV-1 coreceptor is complex and varies according to the viral envelope examined and the various detection system have been used to test the role of the extracellular domain of CCR5, the general conclusions, to date, have been as follows. (A) The *N*-terminus (Nt) and second extracellular loop (ECL-2) play critical roles in gp120 binding and fusion [27, 28]. It has been shown that the negatively charged acidic amino acids and tyrosine residues in the CCR5 Nt (D_2, Y_3, Y_{10}, D_{11}, Y_{14}, Y_{15}, and E_{18}) are important for CD4-dependent gp120-CCR5 binding and viral entry [29-33]. Furthermore, residues in the CCR5 ECL-2 that were found to affect coreceptor function for nonclade B viruses include S_{169}, Q_{170}, K_{171}/E_{172}, Y_{176}, and T_{177} [34], although the dependence of nonclade B viruses on residues in ECL-2 for viral entry may be much higher than that of clade B [31, 33, 35]. (B) All the cysteine residues (C_{20}, C_{101}, C_{178}, and C_{269}) are important for the coreceptor function [34, 36]. In particular, the alanine mutation of cycteine 101 dramatically affected infection efficiency of clade B and non-clade B viruses. This cycteine residue is involved in the formation of a disulfide bond (C_{101}-C_{178}). (C) Posttranslational modifications of CCR5 modulate its function by affecting the affinity of gp120/coreceptor interaction. CCR5 Nt undergoes both *O*-glycosylation and tyrosine sulfation [37]. Serine 6 and serine 7 in Nt are modified by *O*-glycosylation in cell lines and in primary macrophages [38]. The absence of the *O*-glycosylation of CCR5 prevents the binding of CCL3 and CCL4, but has a minimal effect on the efficiency of HIV-1 infection [38]. On the other hand, the prevention of tyrosine sulfation substantially suppressed HIV-1 entry without affecting CCR5 expression [37, 38]. Furthermore, the interaction between soluble gp120-CD4 complexes and CCR5 Nt-based sulfopeptides involves residues located primarily in the V3 stem and the C4 region of gp120 [39, 40], suggesting that the sulfate moieties of tyrosine residues should facilitate electrostatic interactions with positively charged amino acids in the V3 base and the bridging sheet.

Functional Determinants of CXCR4 for HIV-1 Entry

A lot of mutation and chimeric studies of HIV-1 coreceptors have also provided important information on the extracellular domain of CXCR4 involved in the interaction with gp120, although, in contrast to the R5 virus, a region of CXCR4 that plays an important role in viral entry seems to be dispersed in an isolate-dependent manner and more complex. The general conclusions of these studies have been, to date, as follows: (A) Negatively charged acidic amino acids and tyrosine residues dispersed throughout the extracellular domains of CXCR4 are important for X4 viral entry. Multiple single mutations (Y_7, D_{10}, Y_{12}, E_{14}, E_{15}, D_{20}, Y_{21}, D_{22}, E_{26}, E_{32} in Nt and D_{182}, Y_{184}, D_{187}, Y_{190}, D_{193} in ECL-2) affect HIV-1 entry, albeite in an isolate-dependent manner [41-43]. These results show that X4 viral entry mainly depends on tyrosine, aspartate, and glutamate residues (YDE-rich cluster) in Nt and ECL-2. (B) All cysteine residues (C_{28}, C_{109}, C_{186} and C_{274}) are important for the coreceptor function although the alanine mutation of cysteine 274 alone in the third extracellular domain (ECL-3) yielded a CXCR4 molecule possessing an activity nearly 75% of that of the wild type [43]. Alanine mutants of cycteine residues (C_{109} and C_{186}) were essentially undetectable on the cell surface, suggesting that the disruption of disulfide bond formation between cysteine 109 and cysteine 186 results in misfolded CXCR4 molecules that are not well expressed on the cell surface and are important for maintaining coreceptor activity. (C) Like CCR5, CXCR4 is also posttranslationally modified by the sulfation of its amino-terminal tyrosines [44]. However, these finding suggest that the tyrosine sulfate groups at the amino terminus of CXCR4 play a much less important role in the entry of CXCR4-utilizing isolates (CF402.1, SG3, or HXBc2) than the tyrosine sulfate groups of CCR5 in the entry of all CCR5-dependent HIV-1 isolates (JRFL, YU2, and ADA) assayed previously.

Binding Mechanism of CC-Chemokines with CCR5

It is very important to determine which regions of CCR5 are responsible for the specificity of chemokine binding as well as determinants of coreceptor activity. CCR5 natural ligands (CCL3, CCL4, CCL5, and CCL8) are able to inhibit HIV-1 infection *in vivo* [1, 45-49]. Although they are unlikely to bind to identical sites on CCR5, a proposed model for chemokine binding to CCR5 shows a two-step mechanism of receptor activation. As the initial binding step, the Nt domain of CCR5 was shown to be required for chemokine binding, with several charged amino acids and aromatic residues playing a crucial role [29, 50]. In particular, the mutation (D_2, S_7 Y_{10}, D_{11}, and E_{18}) plays an important role in CCL4 binding and the mutation (I_{12}, C_{20}) severely suppressed CCL4 and CCR5 binding [29, 51]. Furthermore, as the second binding step, ECL-2 interacts with the CC-chemokines and confers ligand specificity [52]. Blanpain *et al.* suggested that the mutation (E_{172}, R_{168}, K_{191}) strongly affects CCL3 binding but has little effect on CCL5 binding [53].

Binding Mechanism OF CXC-Chemokine with CXCR4

Crump *et al.* proposed a two-site model for CXCL12-CXCR4 interaction derived from a three-dimensional structure [54]. As an initial docking step, the Nt of CXCR4 interacts with the R-F-F-E-S-H motif of CXCL12. This step leads to conformational changes that allow the subsequent interaction of CXCR4 with the K-P-V-S-L-S-Y-R-C-P-C motif of CXCL12 [55]. Brelot *et al.* [56] and Zhou *et al.* [57] suggested that according to this two-site model for CXCL12-CXCR4, site I involved in CXCL12 binding but not signaling is located in Nt. In particular, glutamamate 14 and/or

glutamate 15, aspartate 20 and tyrosine 21 have importance in the CXCL12 binding. Furthermore, residues required for both CXCL12 binding and signaling at site II were identified in ECL-2 (E_{187}) [56] and ECL-3 (E_{268}) [57]. On the other hand, aspartate 181, aspartate 182, arginine 183 and tyrosine 184 in UPA have no effect on CXCL12 binding as well as intracellular Ca^{2+} influx [56, 57]. Therefore, UPA may be an attractive target for developing peptide-based vaccines that induce anti-CXCR4 Abs with little effect on CXCR4 signaling.

Sequence Identity of Undecapeptidyl Arch Among CC and CXC Receptor Family Members and Among Various Species

Seven-transmembrane domain receptors, such as CCR5 and CXCR4, can exhibit conformational heterogeneity [58]. Therefore, the extracellular domain of those receptors that exists in antigenically same state may be suitable for an antigen based on the chemokine receptor. In our study, UPA was selected as the target because cysteine residues (C_{101} and C_{178}) in ECL-1 and ECL-2 form a rigid disulfide bond and UPA is one of the domains with which the HIV-1 env protein interacts [34, 41-43]. Furthermore, each amino acid sequence of UPA (UPAs: R_{168}-C_{178} in CCR5, N_{176}-C_{186} in CXCR4) is specific among each chemokine receptor family member and is highly conserved in the primates and nonprimates as shown in Fig. (**1**). These results suggest that each UPA in CCR5 or CXCR4 is a suitable target for eliciting autoantibodies against each receptor.

Benefits of Peptide Cycloimmunogen

The benefits of using a peptide immunogen are generally as follows: (i) its immunogenicity can be controlled by polymerization or conjugation with small carrier molecules such as a multiple-antigen peptide (MAP) [59], (ii) it can induce Abs against a very restricted region that includes biologically active epitope, and (iii) its chemical purity can be exactly defined and is cost-effective to produce [60, 61]. However, the mimicry of the conformation of native protein is the most important for inducing an Ab against the conformational epitope of an antigen. Hence, an Ab induced by a linear peptide could recognize a denatured protein but could not recognize the native protein. On the other hand, an Ab that recognizes the conformational epitope of an antigen could not recognize a denatured protein. Indeed, the anti-CXCR4 Ab 12G5 induced by the immunization of Sup-T1 cells that are chronically infected with SIVmac variant CP-MAC [62], could recognize cell surface CXCR4 as deter-

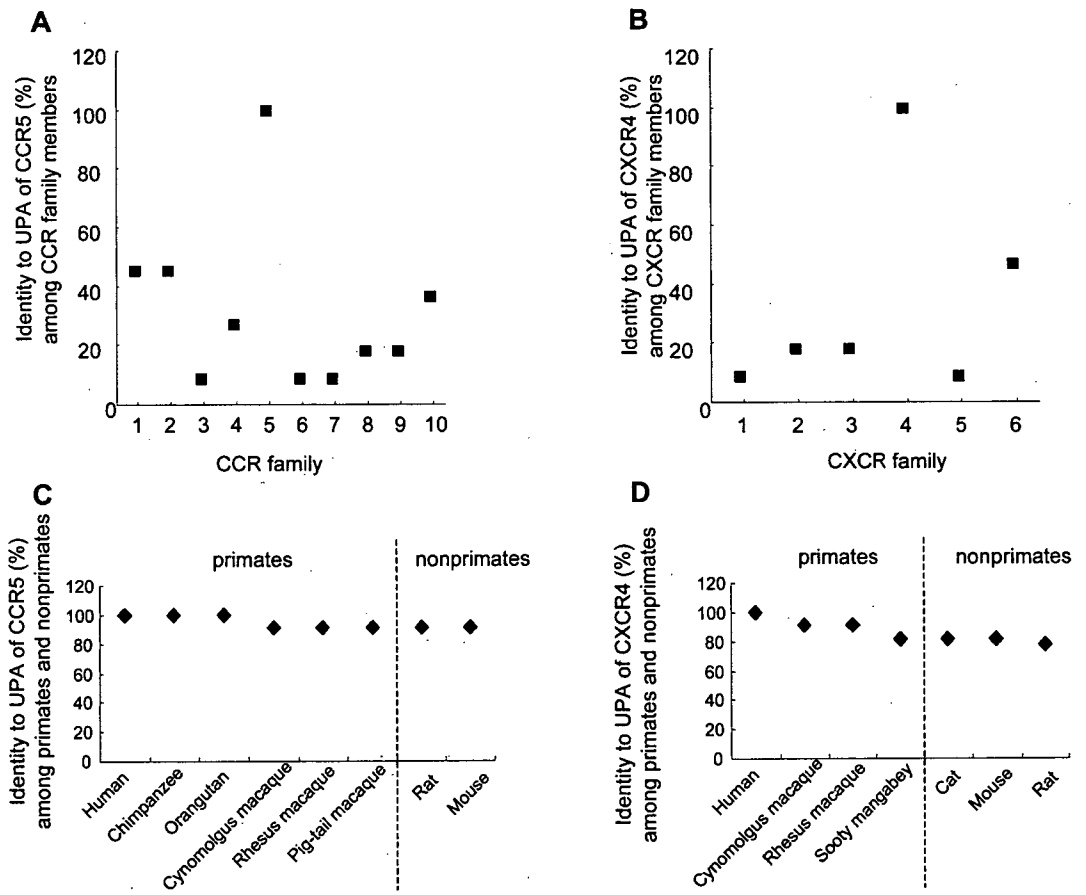

Fig. (1). (A) Sequence identity to CCR5 UPA among UPAs of CCR family. % identity is set to 100 when aligned sequences are 100% identical to the UPA of CCR5. (B) Sequence identity to CXCR4 UPA among UPAs of CXCR family. % identity is set to 100 when aligned sequences are 100% identical to the UPA of CXCR4. (C) Sequence identity to human CCR5 UPA among primates and nonprimates. % identity is set to 100 when aligned sequences are 100% identical to the UPA of CCR5. (D) Sequence identity to human CXCR4 UPA among primates and nonprimates. % identity is set to 100 when aligned sequences are 100% identical to the UPA of CXCR4.

mined by fluorescence-activated cell sorting analysis but could not detect denatured CXCR4 as determined by Western blot analysis. In our study, the peptide antigen was cyclized not by a disulfide bond but by a peptide bond because the conformational stability of a peptide antigen *in vivo* is also a key factor for generating Abs against the native protein. The peptide bond is more robust and stable than a disulfide bond for cyclization. Szewczuk *et al.* suggested that a cyclic peptide antigen is more resistant to proteolytic degradation as shown in their study of a thrombin-specific inhibitor [63]. Thus, the cyclopeptide is more suitable for a linear peptide to not only mimic the native conformational epitope of UPA in CCR5 and CXCR4, but also enhance immunogenicity itself by becoming resistant to proteolytic degradation.

Design and Synthesis of Cycloimmunogens

In our study, three cycloimmunogens were designed for eliciting autoantibodies against CCR5, CXCR4, or both. The hypothetical structural model of CCR5 and CXCR4 is based on its homology with rhodopsin [64], and energy-minimized using the molecular operating environment, (MOE, Chemical Computing Group Inc., Montreal, Quebec, Canada), Figs. (2) and (3) [65, 66]. The ECL-2 region of CCR5 has a unique arch consisting of 11 amino acid residues (UPA) formed on the basis of the cysteine 178 residue bound to a cysteine 101 residue of ECL-1 by a disulfide bond, Fig. (**2A**). The cDDR5 moiety designed to mimic the native conformational epitope of UPA was generated by the cyclization of a decapeptide (R_{168}SQKEGLHYT_{177}) derived from the UPA sequence by the insertion of a spacer-armed dipeptide (Gly-Glu) (shown in green in Fig. (**2B**)). The deduced structure of cDDR5 (shown in red) was adopted to the structural model of UPA in CCR5 using the MOE-Align tool (Chemical Computing Group Inc., Montreal, Quebec, Canada, shown in yellow in Fig. (**2B**)).

On the other hand, the ECL-2 region of CXCR4 also has a unique arch consisting of 11 amino acid residues (UPA) formed on the basis of the cysteine 186 residue bound to the cysteine 109 residue of ECL-1 by a disulfide bond, Fig. (**3A**). The cDDX4 moiety was also generated by the cyclization of a decapeptide (N_{176}VSEADDRYI_{185}) by the insertion of a spacer-armed dipeptide (Gly-Asp) (shown in green in Fig. (**3B**)). The deduced structure of cDDX4 (shown in purple) was adopted to the structural model of UPA in CXCR4 using the MOE-Align tool (Chemical Computing Group Inc., Montreal, Quebec, Canada, shown in yellow in Fig. (**3B**)). The cyclization of the linear peptide was confirmed by MALDI-TOF-MS [65, 66].

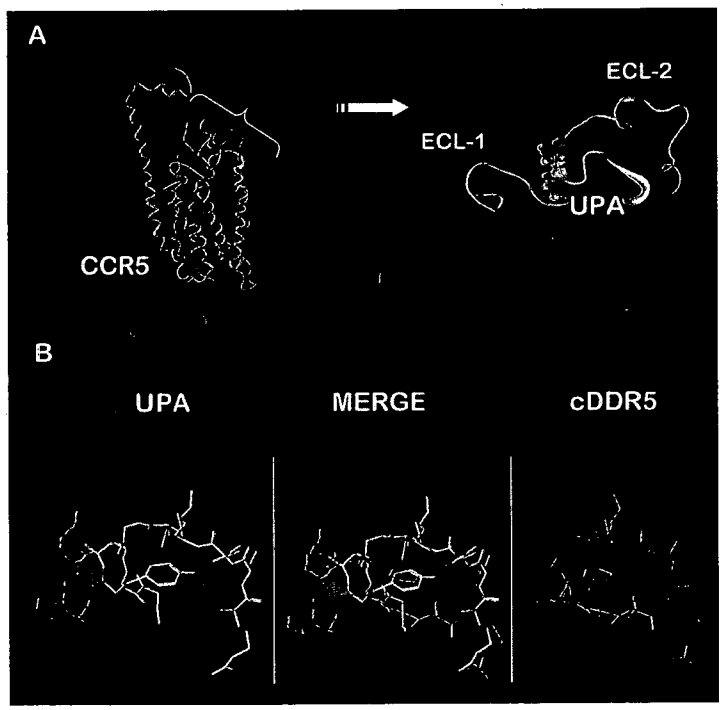

Fig. (2). Deduced structure of UPA in ECL-2 of CCR5. (A) Deduced structure of UPA in extracellular loop-2 of CCR5. The predicted model of CCR5 was constructed using the segmented approach, and MOE was used for actual calculation. The determined structure of rhodopsin was used as the template [64]. Transmembrane helixes are in cyan. The extracellular loops of CCR5 are color-coded: N terminus, purple; extracellular loop-1, green; extracellular loop-2, yellow-orange; UPA, yellow; and extracellular loop-3, magenta. The intercellular loops are in gray, and the C terminus is in red. Because cysteine residues in extracellular loop-1 and extracellular loop-2 form a disulfide bond, the extracellular loop-2 region of CCR5 has a unique arch structure consisting of 11 amino acid residues (yellow). In this study, UPA was selected as the target of peptide immunogens. (B) To mimic the deduced conformational epitope of UPA in CCR5, the decapeptide (R_{168}SQKEGLHYT_{177}) derived from the UPA sequence was cyclized by inserting the spacer-armed dipeptide (Gly-Glu in green), and the deduced structure of cDDR5 (in red) was adopted as the deduced structural model of UPA (in yellow) in CCR5 using the MOE-Align tool.

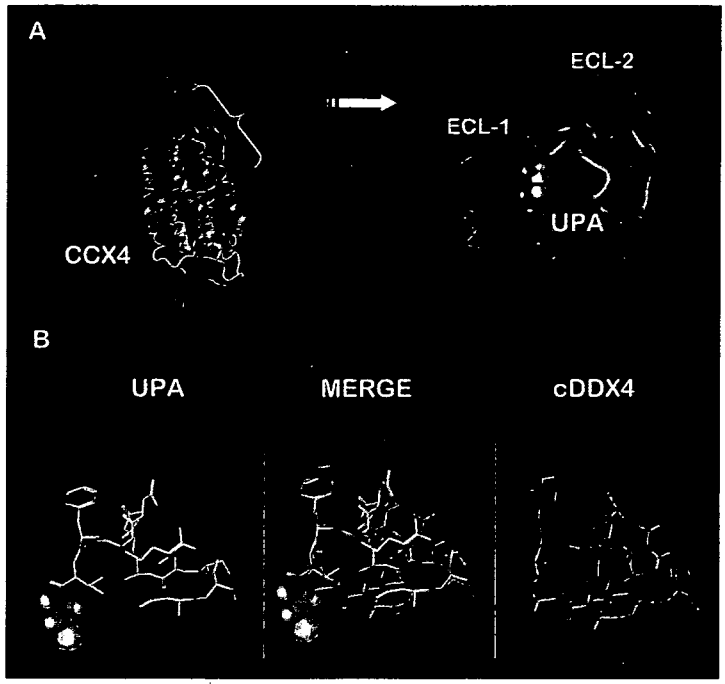

Fig. (3). Deduced structure of UPA in ECL-2 of CXCR4. (A) The predicted model of CXCR4 was constructed using the segmented approach, and MOE was used for actual calculation. The determined structure of rhodopsin was used as the template [64]. Transmembrane helixes are indicated in cyan. The extracellular loops of CXCR4 are color-coded: amino terminus, purple; ECL-1, green; ECL-2, yellow and orange; UPA, yellow; and ECL-3, magenta. The intercellular loops are indicated in white and the C terminus in red. Because cysteine residues in ECL-1 and ECL-2 form a disulfide bond, the ECL-2 region of CXCR4 has a unique arch structure consisting of 11 amino acid residues (UPA, undecapeptidyl arch, yellow). In this study, UPA was selected as the target of peptide immunogens. (B) To mimic the native conformational epitope of UPA in CXCR4, the decapeptide (N_{176}VSEADDRYI$_{185}$) derived from the UPA sequence was cyclized by the insertion of the spacer-armed dipeptide (Gly-Asp in green), and the deduced structure of cDDX4 (in purple) was adopted to the structural model of UPA (in yellow) in CXCR4 using the MOE-Align tool.

Furthermore, a cyclic chimeric dodecapeptide (cCD) mimicking the conformation-specific domains of CCR5 and CXCR4 was also prepared in which Gly-Asp links the amino and carboxyl termini of two combined pentapeptides (S_{169}-G_{173} of CCR5; E_{179}-R_{183} of CXCR4) to elicit the bifunctional Abs against CCR5 and CXCR4, Fig (**4**) [67, 68].

Finally, these cycloimmunogens were conjugated with MAP through the formation of the peptide bound between the beta- or gamma-carboxyl group of aspartate or glutamate within the spacer-armed dipeptide and the amino group within MAP for the immunization of BALB/c mice and cynomolgus macaques [65-67]. MAP, which is composed of a

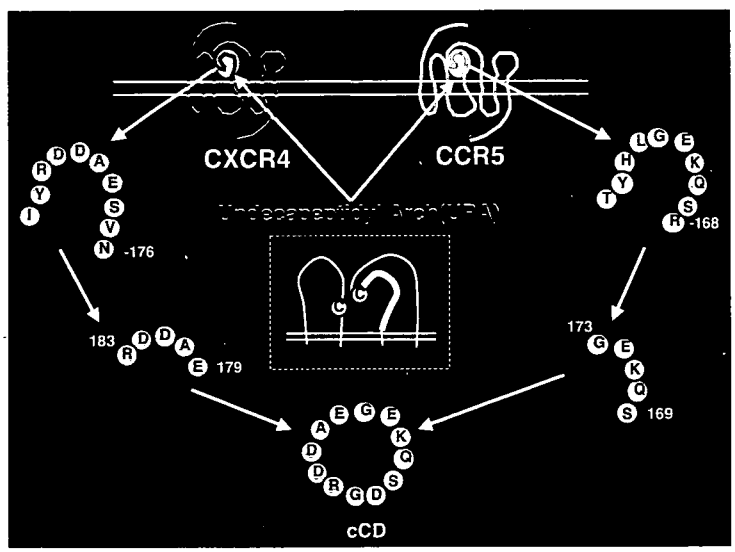

Fig. (4). Overview of preparation of cyclic chimeric peptide (cCD). cCD was constructed with a spacer-armed Gly-Asp dipeptide (in yellow) and two pentapeptides of UPA in ECL-2 derived from CCR5 (in light blue) and CXCR4 (in red).

twofold bifurcating polylysine core developed as a carrier of a peptide antigen, is capable of eliciting a strong Ab response in mice, monkeys, and humans [59].

ESTIMATION OF CHEMOKINE RECEPTOR-BASED HIV-1 VACCINE

Induction of Autoantibodies After Immunization with Chemokine Receptor-Based Cycloimmunogen in BALB/C Mice

One clone, KB8C12, producing the Ab to the UPA-based cycloimmunogen cDDR5-MAP, was effectively selected and purified [69]. To estimate the immunochemical specificity of KB8C12, a BIAcore biosensor bound with biotinylated cDDR5 was used. The result showed that the response of the biotinylated-cDDR5-bound biosensor was enhanced with increasin g concentration of the flowing Ab and that Ab-binding was competed by cDDR5 but not by linear DDR5 composed of the same amino acid residues, as shown in Table **1**. These results suggest that the cycloimmunogen is useful for mimicking the conformational epitope of the targeted region. Furthermore, the binding of KB8C12 to cells expressing CCR5 was determined using a flow cytometer [69]. These results taken together indicate that the Ab to cDDR5-MAP is conformation-specific and recognizes the conformation-specific domain of the UPA of ECL-2 in CCR5.

Moreover, the immunization of BALB/c mice with cDDX4-MAP or cCD-MAP also induces the autoantibodies production [65, 67]. As shown in Table **1**, the immunochemical specificities of the autoantibodies raised by cDDX4-MAP and cCD-MAP are summarized. Interestingly, the immunization of BALB/c mice with cCD-MAP induces the production of bifunctional Abs, CPMAb-I to CPMAb-VII.

Antiviral Activity of Monoclonal Antibodies Elicited by Chemokine Receptor-Based Cycloimmunogens

The anti-HIV-1 activity of KB8C12 was determined using MAGIC-5 cells [69, 70]. As expected, KB8C12 markedly suppressed infection by JRFL, but not by LAV-1, in a dose-dependent manner, and infection by R5 of clade A, C, and E (Table **1**).

Moreover, the anti-HIV activity of IA2-F9 or CPMAb-I to CPMAb-VII was also determined by an infection assay using MAGIC-5 cells [65, 67, 70]. The anti-HIV activities are summarized in Table **1**. Interestingly, CPMAb-I to CPMAb-VII inhibited HIV-1 infection in a clone-dependent manner. Therefore, these results indicate that Abs raised

Table 1. Induction of Autoantibodies After Immunization with Cycloimmunogen in Balb/c Mice and Antiviral Activities

Antigen	Clone	Ab-binding competition[a]		Flow cytometric analysis[b]		Anti-HIV activity[c]			
		Cycloimmunogen	Linear immunogen	CCR5	CXCR4	Clade B (Laboratory strain)		Non-clade B (Primary strain)	
						R5	X4	R5	X4
cDDR5-MAP	KB8C12	+	-	+	-	+	-	+ (A, C, E)	-
cDDX4-MAP	IA2-F9	+	-	-	+	-	+	ND[d]	ND[d]
cCD-MAP	CPMAb-I	ND[d]	ND[d]	+	+	+	+	+ (E)	-
cCD-MAP	CPMAb-II	ND[d]	ND[d]	+	+	+	+	-	-
cCD-MAP	CPMAb-III	ND[d]	ND[d]	+	+	+	-	-	+ (C)
cCD-MAP	CPMAb-IV	ND[d]	ND[d]	+	+	-	-	+ (A, C, E)	-
cCD-MAP	CPMAb-V	ND[d]	ND[d]	+	+	-	-	+ (A, E)	+ (E)
cCD-MAP	CPMAb-VI	ND[d]	ND[d]	+	+	+	-	+ (A, C)	+ (A, C, E)
cCD-MAP	CPMAb-VII	ND[d]	ND[d]	+	+	+	+	+ (A, E)	+ (A, C, E)

a) To estimate the immunochemical specificity of antoantibodies raised from each cycloimmunogen, a BIAcore biosensor bound with biotinylated cycloimmunogen was used as described in refs. [65, 69]. For Ab-binding competition assay, cycloimmunogens (cDDR5, cDDX4) or linear immunogens (linear DDR5, linear DDX4) were used as competitors. + indicates that the binding of KB8C12 or IA2-F9 is competed by only cDDR5 or cDDX4.

b) The binding of autoantibodies to cells expressing CCR5 or CXCR4 was determined using a flow cytometer as described in refs. 65, and 69. + indicates that the autoantibody recognizes native CCR5- or CXCR4-expressing cells.

c) The anti-HIV-1 activity of autoantibodies was determined using MAGIC-5 cells as described in refs. 65, 67, 69, and 70. These cells were separately inoculated with various strains of HIV-1 (clade B: R5 HIV-1 strain JRFL and X4 HIV-1 strain LAV-1; non-clade B: 93RW004 (R5 of clade A), MJ4 (R5 of clade C), 92TH009 (R5 of clade E), 92UG029 (X4 of clade A), 98IN017 (X4 of clade C) and CMU08 (X4 of clade E)) in the presence of the autoantibody. + indicates that the anti-HIV-1 activity is more than 50%. The clade of the primary isolate affected are shown in parentheses.

d) Not determined.

against cCD-MAP have a potent and broad-spectrum inhibitory activity against primary isolates.

Immunogenicity of Chemokine Receptor-Based Cycloimmunogens in Cynomolgus Macaques

To verify whether cDDR5-MAP can induce CCR5-specific Abs with anti-HIV-1 activity in nonhuman primates, an experiment was performed using cynomolgus macaques [66]. Three cynomolgus macaques were immunized with cDDR5-MAP in CFA or IFA by i.p. or s.c. injection according to our immunization schedule. Another three cynomolgus macaques were immunized with MAP as the control. cDDR5-specific Abs were significantly induced in the sera from cynomolgus macaques. The binding of the cDDR5-specific Abs was competed in the case of pretreatment with cDDR5, Fig. (**5A**). The sera showed the immunofluorescence staining of CEM-CCR5 cells, compared with preimmunization sera from these macaques and competed with 2D7 binding, Fig. (**5B**). In contrast, the immunization of

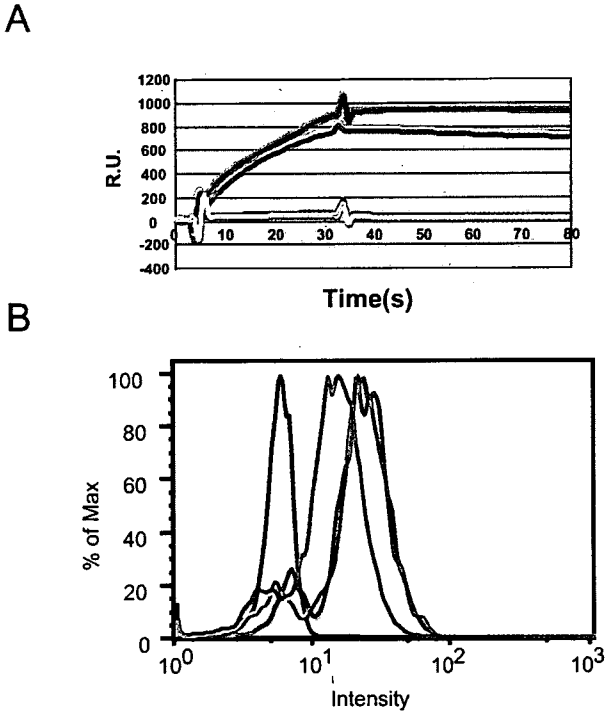

Fig. (5). (A) Immunochemical specificity of anti-cDDR5-specific Abs in sera from cynomolgus macaques. Binding specificity was determined by real-time biomolecular interaction analysis using surface plasmon resonance with a BIAcore biosensor coating biotinylated cDDR5. Antigen-Ab binding and competitive experiments were carried out with serum treated without (blue line) or with cDDR5 (0.1 (green line), 1 (red line), or 10 mmol (light blue)). (B) Anti-cDDR5 specific Abs elicited in cynomolgus macaques compete with 2D7. CEM-CCR5 cells were separately incubated with 2D7 (1 μg) in the absence (blue line) or presence of the preimmunization (green line) or 8 weeks postinitial immunization sera (orange line), and an isotype-matched IgG Ab (control; 1 μg; red line) at 4°C. Then the cells were washed with the washing buffer and resuspended in washing buffer containing FITC-conjugated anti-mouse IgG. The cells were analyzed using an EPICS XL flow cytometer.

cynomolgus macaques with MAP did not induce cDDR5-specific Abs. Furthermore, the anti-HIV-1 activity of sera from cDDR5-MAP immunized macaques was determined using MAGIC-5 cells expressing CCR5 [66]. The cells were separately inoculated with two laboratory strains of clade B HIV-1 (JRFL and LAV-1) or R5 nonclade B HIV-1 primary isolates (clade A: HIV93RW004 and clade C:HIVMJ4) in the presence or absence of immune sera. As expected, the sera from cDDR5-MAP-immunized cynomolgus macaques markedly suppressed infection by HIV-1 (JRFL) in a dose-dependent manner and also suppressed infection by R5 nonclade B HIV-1 primary isolates [66].

We also verified whether cDDX4-MAP can induce CXCR4-specific Abs with anti-HIV-1 activity in nonhuman primates as well as rodents [65]. As expected, cDDX4-bound Abs were detected in the sera from three monkeys 10 weeks postinitial immunization (wpim). However, the sera from two of three cDDX4-MAP-immunized monkeys significantly inhibited HIV-1 infection whereas the serum from one monkey did not, as shown by the comparison between monkeys 0 and 10 wpim. On the other hand, all sera from cDDX4-MAP-immunized monkeys at 27 wpim inhibited HIV-1 replication after boosting at 25 wpim.

Interestingly, the immunization of cynomolgus macaques with cCD-MAP induced cCD-specific Abs in the antisera within, at the most, 6 wpim, although some differences in cCD-specific Ab induction were observed among the macaques [67]. The antisera sampled after immunization specifically recognized CCR5- and CXCR4-expressing MAGIC-5 cells, and inhibited HIV-1 infection by the R5 and X4 laboratory strains of clade B and broadly inhibited infection by HIV-1 primary isolates of nonclade B (93RW004, MJ4, 92TH009, 92UG029, 98IN017 and CMU08, respectively). These results suggest that cCD-MAP induces Abs capable of protecting cross-clade HIV-1 infection.

Protection Against Simian/Human Immunodeficiency Virus Intravenous Challenge

The SHIV-$1_{SF162P3}$ bulk isolate is a pathogenic CCR5-specific simian/human immunodeficiency virus (SHIV) in rhesus macaques [71]. Because sera from cDDR5-MAP-immunized macaques significantly suppressed the infection of MAGIC-5 cells and CEM-CCR5 cells by the SHIV-$1_{SF162P3}$ bulk isolate, all of the MAP- and cDDR5-MAP-immunized macaques were i.v. challenged with 1 ml of 10 $TCID_{50}$/ml $SHIV_{SF162P3}$ five weeks after the third immunization [66]. The course of acute viral infection was monitored by measuring plasma viral RNA load in acutely infected macaques, Fig. (**6**). All of the three control macaques developed detectable plasma viremia, as demonstrated by viral peaks between 1 x 10^9 and 3 x 10^9 viral RNA copies/ml plasma, and sustained plasma viremia at >10^8 viral RNA copies/ml plasma for 3 weeks (1-4 weeks postchallenge). Furthermore, we compared the geometric mean plasma viral RNA loads of the vaccinated and control groups to monitor the effectiveness of vaccination. There were differences of ~19.95- to 217.10-fold in the geometric mean viral loads of the two groups between 1 and 4 weeks postchallenge, Fig. (**6**). However, previous study demonstrated that the immunization with cDDR5-MAP induced anti-cDDR5 serum pro-

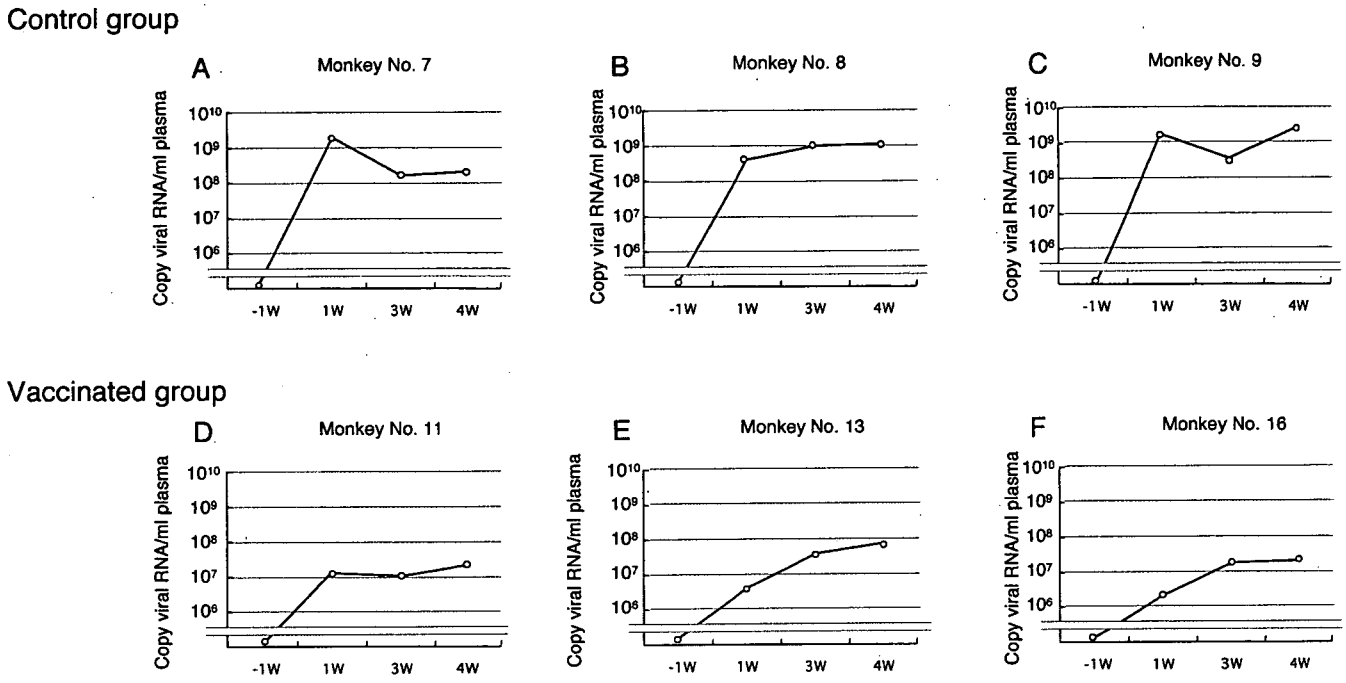

Fig. (6). (A) Intravenous challenge with $SHIV_{SF162P3}$. Whole-blood samples were collected at -1, 1, 3, and 4 week postchallenge, and the samples were examined for plasma viremia. Viral RNA was extracted from macaque plasma and then reverse-transcribed. The resulting cDNA duplicates were amplified by quantitative real-time PCR, as described in Materials and Methods [66].

duction for about 15 weeks after the third immunization although the titer of anti-cDDR5 sera declined over time until 21 wpim [66]. Taken together, these results suggest that the viral load in cDDR5-MAP-vaccinated macaques following a challenge with $SHIV_{SF162P3}$ can be controlled for a longer time when the anti-CCR5 Ab continues to be strongly induced by vaccination for a longer time.

We are currently investigating whether cDDX4- and cCD-MAP vaccination can protect against simian/human immunodeficiency virus challenge.

Effects of Boosting

We assessed whether revaccination is successful at boosting the anti-cDDR5 response. Unfortunately, the anti-cDDR5 Ab was not detected at 25 wpim, but revaccination at 25 weeks with cDDR5-MAP in complete Freund's adjuvant was successfully boosted the Ab response against cDDR5-MAP, Fig. (7). These results suggest that the UPA-based cycloimunogen strategy efficiently breaks B-cell tolerance and the titer of anti-cDDR5 sera was maintained by effective boostings.

On the other hand, cynomolgus macaques are immunized with cDDX4-MAP or cCD-MAP as well as cDDR5-MAP using the same vaccination protocol. The revaccination with cDDX4-MAP in complete Freund's adjuvant was also effectively boosted the Ab response against cDDX4-MAP. Interestingly, the immunization with cCD-MAP induced a longer-term production of anti-cCD serum, that is, for ~72 weeks after the third immunization and the revaccination with cCD-MAP in complete Freund's adjuvant was also successful at boosting the Ab response against cCD-MAP. These results suggest that cCD-MAP is one of the attractive mimotope peptide antigens for circumventing the tolerance mechanisms that the immune system has developed to normally block the maturation of B cells specific for self-antigens.

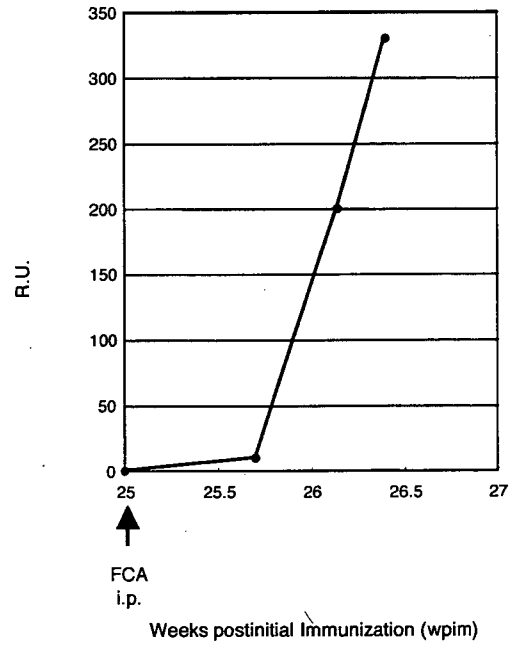

Fig. (7). Effects of boosting at 25 weeks postinitial immunization. The anti-cDDR5-specific Abs from serum were detected by real-time biomolecular interaction analysis using surface plasmon resonance with a biotinylated cDDR5-bound BIAcore biosensor, as shown in Fig. (5). The highest response units (R.Us.) are plotted.